W^+W^- boson pair production in proton-proton collisions at $\sqrt{s} = 13$ TeV

A. M. Sirunyan *et al.*[*]

(CMS Collaboration)

A measurement of the W^+W^- boson pair production cross section in proton-proton collisions at $\sqrt{s} = 13$ TeV is presented. The data used in this study are collected with the CMS detector at the CERN LHC and correspond to an integrated luminosity of 35.9 fb^{-1}. The W^+W^- candidate events are selected by requiring two oppositely charged leptons (electrons or muons). Two methods for reducing background contributions are employed. In the first one, a sequence of requirements on kinematic quantities is applied allowing a measurement of the total production cross section, 117.6 ± 6.8 pb, which agrees well with the theoretical prediction. Fiducial cross sections are also reported for events with zero or one jet, and the change in the zero-jet fiducial cross section with the jet transverse momentum threshold is measured. Normalized differential cross sections are reported within the fiducial region. A second method for suppressing background contributions employs two random forest classifiers. The analysis based on this method includes a measurement of the total production cross section and also a measurement of the normalized jet multiplicity distribution in W^+W^- events. Finally, a dilepton invariant mass distribution is used to probe for physics beyond the standard model in the context of an effective field theory, and constraints on the presence of dimension-6 operators are derived.

I. INTRODUCTION

The standard model (SM) description of electroweak and strong interactions can be tested through measurements of the W^+W^- boson pair production cross section at a hadron collider. Aside from tests of the SM, W^+W^- production represents an important background for new particle searches. The W^+W^- cross section has been measured in proton-antiproton collisions at $\sqrt{s} = 1.96$ TeV [1,2] and in proton-proton (pp) collisions at 7 and 8 TeV [3–6]. More recently, the ATLAS Collaboration published measurements with pp collision data at 13 TeV [7].

The SM production of W^+W^- pairs proceeds mainly through three processes: the dominant $q\bar{q}$ annihilation process; the $gg \to W^+W^-$ process, which occurs at higher order in perturbative quantum chromodynamics (QCD); and the Higgs boson process $H \to W^+W^-$, which is roughly 10 times smaller than the other processes and is considered a background in this analysis. A calculation of the W^+W^- production cross section in pp collisions at $\sqrt{s} = 13$ TeV gives the value $118.7^{+3.0}_{-2.6}$ pb [8]. This calculation includes the $q\bar{q}$ annihilation process calculated

at next-to-next-to-leading order (NNLO) precision in perturbative QCD and a contribution of 4.0 pb from the $gg \to W^+W^-$ gluon fusion process calculated at leading order (LO). The uncertainties reflect the dependence of the calculation on the QCD factorization and renormalization scales. For the analysis presented in this paper, the $gg \to W^+W^-$ contribution is corrected by a factor of 1.4, which comes from the ratio of the $gg \to W^+W^-$ cross section at next-to-leading order (NLO) to the same cross section at LO [9]. A further adjustment of -1.2% for the $q\bar{q}$ annihilation process is applied to account for electroweak corrections [10]. Our evaluation of uncertainties from parton distribution functions (PDFs) and the strong coupling α_S amounts to 2.0 pb. Taking all corrections and uncertainties together, the theoretical cross section used in this paper for the inclusive W^+W^- production at $\sqrt{s} = 13$ TeV is $\sigma_{\text{tot}}^{\text{NNLO}} = 118.8 \pm 3.6$ pb.

This paper reports studies of W^+W^- production in pp collisions at $\sqrt{s} = 13$ TeV with the CMS detector at the CERN LHC. Two analyses are performed using events that contain a pair of oppositely charged leptons (electrons or muons); they differ in the way background contributions are reduced. The first method is based on techniques described in Refs. [4–6]; the analysis based on this method is referred to as the "sequential cut analysis." A second, newer approach makes use of random forest classifiers [11–13] trained with simulated data to differentiate signal events from Drell-Yan (DY) and top quark backgrounds; this analysis is referred to as the "random forest analysis."

The two methods complement one another. The sequential cut analysis separates events with same-flavor (SF) or different-flavor (DF) lepton pairs and also events with zero or one jet. As a consequence, background contributions from the Drell-Yan production of lepton pairs can be controlled. Furthermore, the impact of theoretical uncertainties due to missing higher-order QCD calculations is kept under control through access to both the zero- and one-jet final states. The random forest analysis does not separate SF and DF lepton pairs and does not separate events with different jet multiplicities. Instead, it combines kinematic and topological quantities to achieve a high sample purity. The contamination from top quark events, which is not negligible in the sequential cut analysis, is significantly smaller in the random forest analysis. The random forest technique allows for flexible control over the top quark background contamination, which is exploited to study the jet multiplicity in W^+W^- signal events. However, the sensitivity of the random forest to QCD uncertainties is significantly larger than that of the sequential cut analysis, as discussed in Sec. IX A.

Total W^+W^- production cross sections are reported in Sec. IX A for both analyses based on fits to the observed yields. Cross sections in a specific fiducial region are reported in Sec. IX B for the sequential cut analysis; these cross sections are separately reported for $W^+W^- \to \ell^+\nu\ell^-\bar{\nu}$ events with zero or one jet (ℓ refers to electrons and muons). Also, the change in the zero-jet W^+W^- cross section with variations in the jet transverse momentum (p_T) threshold is measured.

Normalized differential cross sections within the fiducial region are also reported in Sec. X. The normalization reduces both theoretical and experimental uncertainties. The impact of experimental resolutions is removed using a fitting technique that builds templates of reconstructed quantities mapped onto generator-level quantities. Comparisons to NLO predictions are presented.

The distribution of exclusive jet multiplicities for W^+W^- production is interesting given the sensitivity of previous results to a "jet veto" in which events with one or more jets were rejected [2–4,6]. In Sec. XI, this paper reports a measurement of the normalized jet multiplicity distribution based on the random forest analysis.

Finally, the possibility of anomalous production of W^+W^- events that can be modeled by higher-dimensional operators beyond the dimension-4 operators of the SM is probed using events with an electron-muon final state. Such operators arise in an effective field theory expansion of the Lagrangian and each appears with its own Wilson coefficient [14,15]. Distributions of the electron-muon invariant mass $m_{e\mu}$ are used because they are robust against mismodeling of the W^+W^- transverse boost and are sensitive to the value of the Wilson coefficients associated with the dimension-6 operators. The observed distributions provide no evidence for anomalous events. Limits are placed on the coefficients associated with dimension-6 operators in Sec. XII.

II. THE CMS DETECTOR

The central feature of the CMS apparatus is a superconducting solenoid of 6 m internal diameter, providing a magnetic field of 3.8 T. Within the solenoid volume are a silicon pixel and strip tracker, a lead tungstate crystal electromagnetic calorimeter (ECAL), and a brass and scintillator hadron calorimeter, each composed of a barrel and two end cap sections. Forward calorimeters extend the pseudorapidity (η) coverage provided by the barrel and end cap detectors. Muons are detected in gas-ionization chambers embedded in the steel flux-return yoke outside the solenoid. The first level of the CMS trigger system [16], composed of custom hardware processors, is designed to select the most interesting events within a time interval less than 4 μs, using information from the calorimeters and muon detectors, with the output rate of up to 100 kHz. The high-level trigger processor farm further reduces the event rate to about 1 kHz before data storage. A more detailed description of the CMS detector, together with a definition of the coordinate system used and the relevant kinematic variables, can be found in Ref. [17].

III. DATA AND SIMULATED SAMPLES

A sample of pp collision data collected in 2016 with the CMS experiment at the LHC at $\sqrt{s} = 13$ TeV is used for this analysis; the total integrated luminosity is 35.9 ± 0.9 fb^{-1}.

Events are stored for analysis if they satisfy the selection criteria of online triggers [16] requiring the presence of one or two isolated leptons (electrons or muons) with high p_T. The lowest p_T thresholds for the double-lepton triggers are 17 GeV for the leading lepton and 12 (8) GeV when the trailing lepton is an electron (muon). The single-lepton triggers have p_T thresholds of 25 and 20 GeV for electrons and muons, respectively. The trigger efficiency is measured using $Z \to \ell^+\ell^-$ events and is larger than 98% for W^+W^- events with an uncertainty of about 1%.

Several Monte Carlo (MC) event generators are used to simulate the signal and background processes. The simulated samples are used to optimize the event selection, evaluate selection efficiencies and systematic uncertainties, and compute expected yields. The production of W^+W^- events via $q\bar{q}$ annihilation ($q\bar{q} \to W^+W^-$) is generated at NLO precision with POWHEG v2 [18–23], and W^+W^- production via gluon fusion ($gg \to W^+W^-$) is generated at LO using MCFM v7.0 [24]. The production of Higgs bosons is generated with POWHEG [23] and $H \to W^+W^-$ decays are generated with JHUGEN v5.2.5 [25]. Events for other diboson and triboson production processes are generated at NLO precision with MADGRAPH 5_AMC@NLO2.2.2 [26]. The same generator is used for simulating $Z +$ jets,

which includes Drell-Yan production, and $W\gamma^*$ event samples. Finally, the top quark final states $t\bar{t}$ and tW are generated at NLO precision with POWHEG [27,28]. The PYTHIA 8.212 [29] package with the CUETP8M1 parameter set (tune) [30] and the NNPDF 2.3 [31] PDF set are used for hadronization, parton showering, and the underlying event simulation. For top quark processes, the NNPDF 3.0 PDF set [32] and the CUETP8M2T4 tune [33] are used.

The quality of the signal modeling is improved by applying weights to the W^+W^- POWHEG events such that the NNLO calculation [8] of transverse momentum spectrum of the W^+W^- system, p_T^{WW}, is reproduced.

For all processes, the detector response is simulated using a detailed description of the CMS detector, based on the GEANT4 package [34]. Events are reconstructed with the same algorithms as for data. The simulated samples include additional interactions per bunch crossing (pileup) with a vertex multiplicity distribution that closely matches the observed one.

IV. EVENT RECONSTRUCTION

Events are reconstructed using the CMS particle-flow (PF) algorithm [35], which combines information from the tracker, calorimeters, and muon systems to create objects called PF candidates that are subsequently identified as charged and neutral hadrons, photons, muons, and electrons.

The primary pp interaction vertex is defined to be the one with the largest value of the sum of p_T^2 for all physics objects associated with that vertex. These objects include jets clustered using the jet finding algorithm [36,37] with the tracks assigned to the primary vertex as inputs and the associated missing transverse momentum vector. All neutral PF candidates and charged PF candidates associated with the primary vertex are clustered into jets using the anti-k_T clustering algorithm [36] with a distance parameter of $R = 0.4$. The transverse momentum imbalance $\vec{p}_\mathrm{T}^{\mathrm{miss}}$ is the negative vector sum of the transverse momenta of all charged and neutral PF candidates; its magnitude is denoted by $p_\mathrm{T}^{\mathrm{miss}}$. The effects of pileup are mitigated as described in Refs. [38,39].

Jets originating from b quarks are identified by a multivariate algorithm called the combined secondary vertex algorithm CSV v2 [40,41], which combines information from tracks, secondary vertices, and low-momentum electrons and muons associated with the jet. Two working points are used in this analysis for jets with $p_\mathrm{T} > 20$ GeV. The "loose" working point has an efficiency of approximately 88% for jets originating from the hadronization of b quarks typical in $t\bar{t}$ events and a mistag rate of about 10% for jets originating from the hadronization of light-flavor quarks or gluons. The "medium" working point has a b-tagging efficiency of about 64% for b jets in $t\bar{t}$ events and a mistag rate of about 1% for light-flavor quark and gluon jets.

Electron candidates are reconstructed from clusters in the ECAL that are matched to a track reconstructed with a Gaussian-sum filter algorithm [42]. The track is required to be consistent with originating from the primary vertex. The sum of p_T of PF candidates within a cone of size $\Delta R = \sqrt{(\Delta\eta)^2 + (\Delta\phi)^2} < 0.3$ around the electron direction, excluding the electron itself, is required to be less than about 6% of the electron p_T. Charged PF candidates are included in the isolation sum only if they are associated with the primary vertex. The average contribution from neutral PF candidates not associated with the primary vertex, estimated from simulation as a function of the energy density in the event and the η direction of the electron candidate, is subtracted before comparing to the electron momentum.

Muon candidates are reconstructed by combining signals from the muon subsystems together with those from the tracker [43,44]. The track reconstructed in the silicon pixel and strip detector must be consistent with originating from the primary vertex. The sum of the p_T of the additional PF candidates within a cone of size $\Delta R < 0.4$ around the muon direction is required to be less than 15% of the muon p_T after applying a correction for neutral PF candidates not associated with the primary vertex, analogous to the electron case.

V. EVENT SELECTION

The key feature of the W^+W^- channel is the presence of two oppositely charged leptons that are isolated from any jet activity and have relatively large p_T. The two methods for isolating a W^+W^- signal, the sequential cut method and the random forest method, both require two oppositely charged, isolated electrons or muons that have sufficient p_T to ensure good trigger efficiency. The lepton reconstruction, selection, and isolation criteria are the same for the two methods as are most of the kinematic requirements detailed below.

The largest background contributions come from the Drell-Yan production of lepton pairs and $t\bar{t}$ events in which both top quarks decay leptonically. Drell-Yan events can be suppressed by selecting events with one electron and one muon (i.e., DF leptons) and by applying a veto of the Z boson resonant peak in events with SF leptons. Contributions from $t\bar{t}$ events can be reduced by rejecting events with b-tagged jets.

Another important background contribution arises from events with one or more jets produced in association with a single W boson. A nonprompt lepton from a jet could be selected with charge opposite to that of the prompt lepton from the W boson decay. This background contribution is estimated with two techniques based on specially selected events. In the sequential cut analysis, the calculation hinges

TABLE I. Summary of the event selection criteria for the sequential cut and the random forest analyses. DYMVA refers to an event classifier used in the sequential cut analysis to suppress Drell-Yan background events. RF refers to random forest classifiers. Kinematic quantities are measured in GeV. The symbol (…) means no requirement applied.

Quantity	Sequential cut		Random forest	
	DF	SF	DF	SF
Number of leptons	Strictly 2		Strictly 2	
Lepton charges	Opposite		Opposite	
$p_T^{\ell\,\mathrm{max}}$	>25		>25	
$p_T^{\ell\,\mathrm{min}}$	>20		>20	
$m_{\ell\ell}$	>20	>40	>30	>30
Additional leptons	0		0	
$|m_{\ell\ell} - m_Z|$	…	>15	…	>15
$p_T^{\ell\ell}$	>30	>30	…	…
p_T^{miss}	>20	>55	…	…
$p_T^{\mathrm{miss,proj}}$, $p_T^{\mathrm{miss,track\ proj}}$	>20	>20	…	…
Number of jets	≤ 1		…	…
Number of b-tagged jets	0		0	
DYMVA score	…	>0.9	…	…
Drell-Yan RF score S_{DY}	…	…	>0.96	
$t\bar{t}$ RF score $S_{t\bar{t}}$	…	…	>0.6	

on the probability for a nonprompt lepton to be selected, whereas in the random forest selection, it depends on a sample of events with two leptons of equal charge.

Except where noted, W^+W^- events with τ leptons decaying to electrons or muons are included as signal.

A. Sequential cut selection

The sequential cut selection imposes a set of discrete requirements on kinematic and topological quantities and on a multivariate analysis tool to suppress Drell-Yan background in events with SF leptons.

The lepton p_T requirements ensure a good reconstruction and identification efficiency: the leading lepton must have $p_T^{\ell\,\mathrm{max}} > 25$ GeV, and the trailing lepton must have $p_T^{\ell\,\mathrm{min}} > 20$ GeV. Pseudorapidity ranges are designed to cover regions of good reconstruction quality: for electrons, the ECAL supercluster must satisfy $|\eta| < 1.479$ or $1.566 < |\eta| < 2.5$ and for muons, $|\eta| < 2.4$. To avoid low-mass resonances and leptons from decays of hadrons, the dilepton invariant mass must be large enough: $m_{\ell\ell} > 20$ GeV. The transverse momentum of the lepton pair is required to satisfy $p_T^{\ell\ell} > 30$ GeV to reduce background contributions from nonprompt leptons. Events with a third, loosely identified lepton with $p_T > 10$ GeV are rejected to reduce background contributions from WZ and ZZ (i.e., VZ) production.

The missing transverse momentum is required to be >20 GeV. In order to make the analysis insensitive to instrumental p_T^{miss} caused by mismeasurements of the lepton momenta, a so-called "projected p_T^{miss}," denoted

$p_T^{\mathrm{miss,proj}}$, is defined as follows. The lepton closest to the $\vec{p}_T^{\mathrm{miss}}$ vector is identified and the azimuthal angle $\Delta\phi$ between the $\vec{p}_T$ of the lepton and $\vec{p}_T^{\mathrm{miss}}$ is computed. The quantity $p_T^{\mathrm{miss,proj}}$ is the perpendicular component of $\vec{p}_T^{\mathrm{miss}}$ with respect to $\vec{p}_T$. When $|\Delta\phi| < \pi/2$, $p_T^{\mathrm{miss,proj}}$ is required to be larger than 20 GeV. The same requirement is imposed using the projected $\vec{p}_T^{\mathrm{miss}}$ vector reconstructed from only the charged PF candidates associated with the primary vertex: $p_T^{\mathrm{miss,track\ proj}} > 20$ GeV.

The selection criteria are tightened for SF final states where the contamination from Drell-Yan events is much larger. Events with $m_{\ell\ell}$ within 15 GeV of the Z boson mass m_Z are discarded, and the minimum $m_{\ell\ell}$ is increased to 40 GeV. The p_T^{miss} requirement is raised to 55 GeV. Finally, a multivariate classifier called DYMVA [45,46] based on a boosted decision tree is used to discriminate against the Drell-Yan background.

Only events with zero or one reconstructed jet with $p_T^J > 30$ GeV and $|\eta^J| < 4.7$ are used in the analysis. Jets falling within $\Delta R < 0.4$ of a selected lepton are discarded. To suppress top quark background contributions, events with one or more jets tagged as b jets using the CSV v2 loose working point and with $p_T^b > 20$ GeV are also rejected.

Table I summarizes the event selection criteria, and Table II lists the sample composition after the fits described in Sec. VII have been executed. Example kinematic distributions are shown in Fig. 1 for events with no jets and in Fig. 2 for events with exactly one jet. The simulations reproduce the observed distributions well.

TABLE II. Sample composition for the sequential cut and random forest selections after the fits described in Sec. VII have been executed; the uncertainties shown are based on the total uncertainty obtained from the fit. The purity is the fraction of selected events that are W^+W^- signal events. "Observed" refers to the number of events observed in the data.

Process	Sequential cut DF 0-jet	DF 1-jet	SF 0-jet	SF 1-jet	Random forest DF	SF
Top quark	2110 ± 110	5000 ± 120	1202 ± 66	2211 ± 69	3450 ± 340	830 ± 82
Drell-Yan	129 ± 10	498 ± 38	1230 ± 260	285 ± 86	1360 ± 130	692 ± 72
VZ	227 ± 13	270 ± 12	192 ± 12	110 ± 7	279 ± 29	139 ± 10
VVV	11 ± 1	29 ± 2	4 ± 1	6 ± 1	13 ± 4	3 ± 2
$H \to W^+W^-$	269 ± 41	150 ± 25	50 ± 2	27 ± 1	241 ± 26	90 ± 10
$W \gamma^{(*)}$	147 ± 17	136 ± 13	123 ± 5	58 ± 6	305 ± 88	20 ± 6
Nonprompt leptons	980 ± 230	550 ± 120	153 ± 39	127 ± 32	940 ± 300	183 ± 59
Total background	3870 ± 260	6640 ± 180	2950 ± 270	2820 ± 120	6600 ± 480	1960 ± 120
	10510 ± 310		5780 ± 300			
$qq \to W^+W^-$	6430 ± 250	2530 ± 140	2500 ± 180	1018 ± 71	12070 ± 770	2820 ± 180
$gg \to W^+W^-$	521 ± 66	291 ± 38	228 ± 32	117 ± 15	693 ± 44	276 ± 17
Total W^+W^-	6950 ± 260	2820 ± 150	2730 ± 190	1136 ± 72	12770 ± 820	3100 ± 200
	9780 ± 300		3860 ± 200			
Total yield	10820 ± 360	9460 ± 240	5680 ± 330	3960 ± 360	19360 ± 950	5060 ± 240
	20280 ± 430		9640 ± 490			
Purity	0.64	0.30	0.48	0.29	0.66	0.61
	0.48		0.40			
Observed	$10\,866$	9404	5690	3914	$19\,418$	5210

B. Random forest selection

A random forest (RF) classifier is an aggregate of binary decision trees that have been trained independently and in parallel [11]. Each individual tree uses a random subset of features which mitigates against overfitting, a problem that challenges other classifiers based on decision trees. The random forest classifier is effective if there are many trees, and the aggregation of many trees averages out potential overfitting by individual trees. A random forest classifier is expected to improve monotonically without overfitting [12] in contrast to other methods. Building a random forest classifier requires less tuning of hyperparameters compared, for example, with boosted decision trees, and its performance is as good [13].

The random forest analysis begins with a preselection that is close to the first set of requirements in the sequential cut analysis. The selection of electrons and muons is identical. To avoid low-mass resonances and leptons from decays of hadrons, $m_{\ell\ell} > 30$ GeV is required for both DF and SF events. To suppress the large background contribution from Z boson decays, events with SF leptons and with $m_{\ell\ell}$ within 15 GeV of the Z boson mass are rejected. Events with a third, loosely identified lepton with $p_T > 10$ GeV are rejected to reduce backgrounds from VZ production. Finally, events with one or more b-tagged jets ($p_T^b > 20$ GeV and medium working point) are rejected, since the background from $t\bar{t}$ production is characterized by the presence of b jets

whereas the signal is not. These requirements are known as the preselection requirements.

After the preselection, the largest background contamination comes from Drell-Yan production of lepton pairs and $t\bar{t}$ production with both top quarks producing prompt leptons. To reduce these backgrounds, two independent random forest classifiers are constructed: an anti-Drell-Yan classifier optimized to distinguish Drell-Yan and W^+W^- signal events, and an anti-$t\bar{t}$ classifier optimized to distinguish $t\bar{t}$ and W^+W^- events. The classifiers produce scores, S_{DY} and $S_{t\bar{t}}$, arranged so that signal appears mainly at $S_{DY} \approx 1$ and $S_{t\bar{t}} \approx 1$ while backgrounds appear mainly at $S_{DY} \approx 0$ and $S_{t\bar{t}} \approx 0$. Figure 3 shows the distributions of the scores for the two random forest classifiers. The signal region is defined by the requirements $S_{DY} > S_{DY}^{min}$ and $S_{t\bar{t}} > S_{t\bar{t}}^{min}$. For the cross section measurement, the specific values $S_{DY}^{min} = 0.96$ and $S_{t\bar{t}}^{min} = 0.6$ are set by simultaneously minimizing the uncertainty in the cross section and maximizing the purity of the selected sample. For measuring the jet multiplicity, a lower value of $S_{t\bar{t}}^{min} = 0.2$ is used, which increases the efficiency for W^+W^- events with jets. A Drell-Yan control region is defined by $S_{DY} < 0.6$ and $S_{t\bar{t}} > 0.6$ and a $t\bar{t}$ control region is defined by $S_{DY} > 0.6$ and $S_{t\bar{t}} < 0.6$. The event selection used in this measurement is summarized in Table I.

The architecture of the two random forest classifiers is determined through an optimization of hyperparameters explored in a gridlike fashion. The optimal architecture for
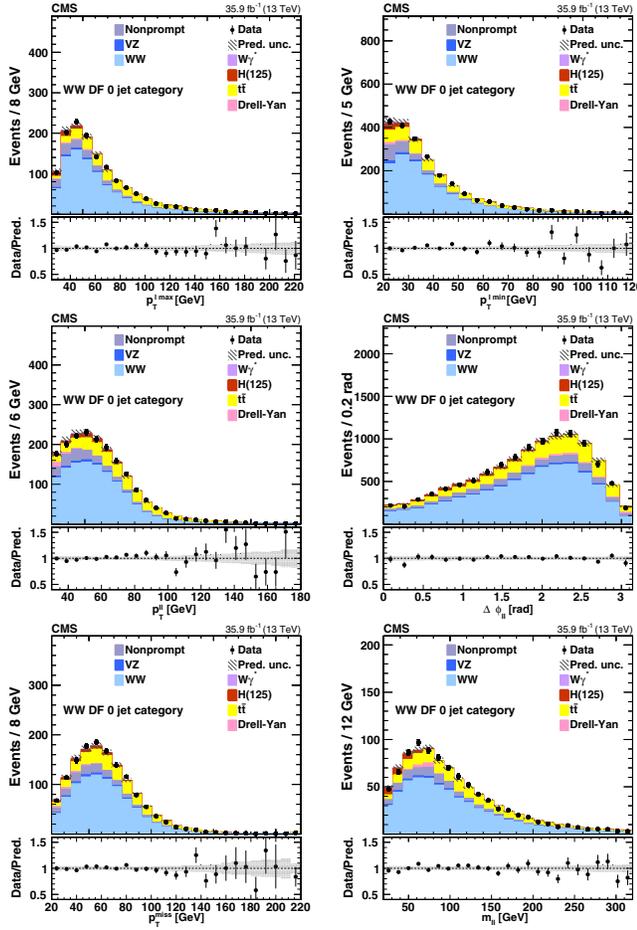
FIG. 1. Kinematic distributions for events with zero jets and DF leptons in the sequential cut analysis. The distributions show the leading and trailing lepton p_T ($p_T^{\ell\,\mathrm{max}}$ and $p_T^{\ell\,\mathrm{min}}$), the dilepton transverse momentum $p_T^{\ell\ell}$, the azimuthal angle between the two leptons $\Delta\phi_{\ell\ell}$, the missing transverse momentum p_T^{miss}, and the dilepton invariant mass $m_{\ell\ell}$. The error bars on the data points represent the statistical uncertainty of the data, and the hatched areas represent the combined systematic and statistical uncertainty of the predicted yield in each bin. The last bin includes the overflow.
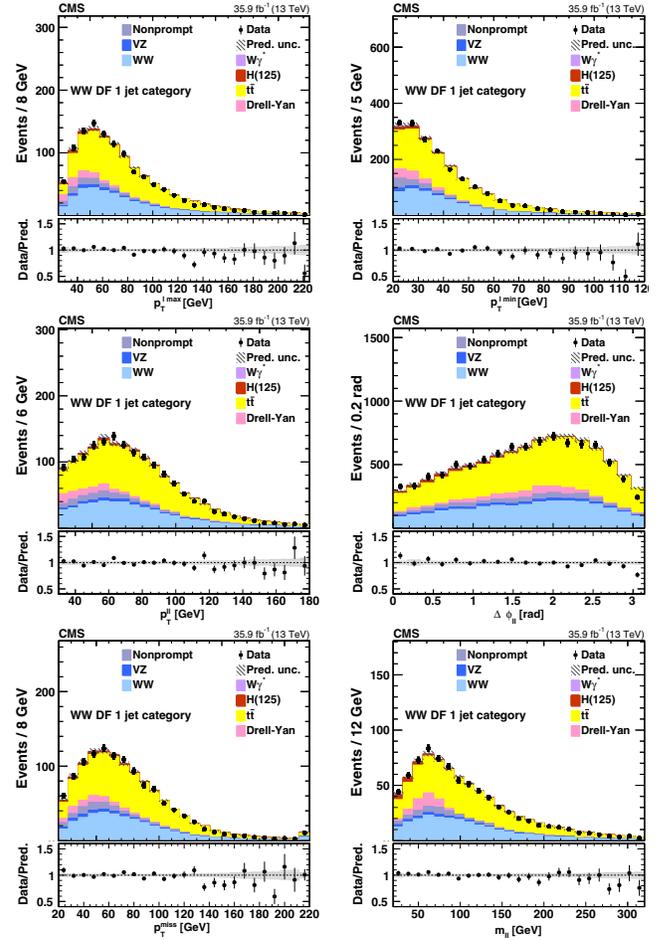
FIG. 2. Kinematic distributions for events with exactly one jet and DF leptons in the sequential cut analysis. The quantities, error bars, and hatched areas are the same as in Fig. 1.

this problem has 50 trees with a maximum tree depth of 20; the minimum number of samples per split is 50 and the minimum number of samples for a leaf is one. The maximum number of features seen by any single tree is the square root of the total number of features (ten for the DY random forest and eight for the $t\bar{t}$ random forest).

The random forest classifier takes as input some of the kinematic quantities listed in Table I and several other event features as listed in Table III. These include the invariant mass of the two leptons and the missing momentum vector $m_{\ell\ell p_T^{\mathrm{miss}}}$, the azimuthal angle between the lepton pair and the missing momentum vector $\Delta\phi_{\ell\ell p_T^{\mathrm{miss}}}$, the smallest azimuthal angle between either lepton and any reconstructed jet $\Delta\phi_{\ell\mathrm{J}}$, and the smallest azimuthal angle between

the missing momentum vector and any jet $\Delta\phi_{p_T^{\mathrm{miss}}\mathrm{J}}$. The random forest classifier also makes use of the scalar sum of jet transverse momenta H_T, and of the vector sum of the jet transverse momenta, referred to as the recoil in the event.

The sample composition for the signal region is summarized in Table II. The signal efficiency and purity are higher than in the sequential cut analysis.

VI. BACKGROUND ESTIMATION

A combination of methods based on data control samples and simulations are used to estimate background contributions. The methods used in the sequential cut analysis and the random forest analysis are similar. The differences are described below.

The largest background contribution comes from $t\bar{t}$ and single top production which together are referred to as top quark production. This contribution arises when b jets are not tagged either because they fall outside the kinematic region where tagging is possible or because they receive low scores from the CSV v2 b-tagging algorithm.
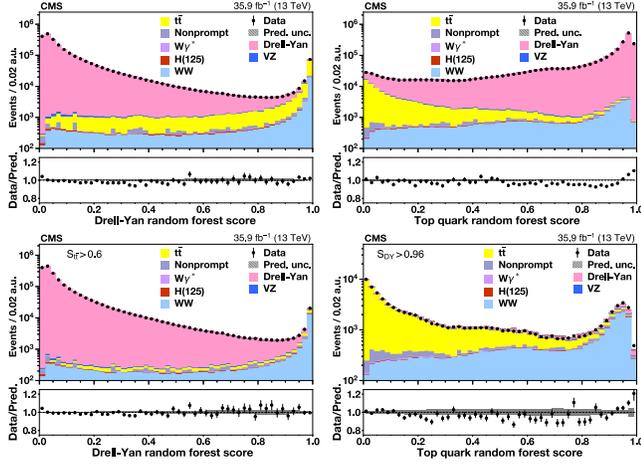
FIG. 3. Top left: score S_{DY} distribution for the Drell-Yan discriminating random forest discriminant. The Drell-Yan distribution peaks toward zero and the W^+W^- distribution peaks toward one. Top right: score $S_{t\bar{t}}$ distribution for the top quark random forest discriminant. The $t\bar{t}$ distribution peaks toward zero and the W^+W^- peaks toward one. Bottom left: the S_{DY} distribution after suppressing top quark events with $S_{t\bar{t}} > S_{t\bar{t}}^{\min} = 0.6$. Bottom right: the $S_{t\bar{t}}$ distribution after suppressing Drell-Yan events with $S_{\mathrm{DY}} > S_{\mathrm{DY}}^{\min} = 0.96$. The error bars on the points represent the statistical uncertainties for the data, and the hatched areas represent the combined systematic and statistical uncertainties of the predicted yield in each bin.

The sequential cut analysis defines a control region by requiring at least one b-tagged jet. The normalization of the top quark background in the signal region is set according to the number of events in this control region. Similarly, the random forest analysis defines a top quark control region

TABLE III. Features used for the random forest classifiers. The first classifier distinguishes Drell-Yan and W^+W^- signal events, and the second one distinguishes top quark events and signal events.

	Classifier	
Feature	Drell-Yan	Top quark
Lepton flavor	✓	
Number of jets		✓
$p_{\mathrm{T}}^{\ell\,\min}$	✓	
$p_{\mathrm{T}}^{\mathrm{miss}}$	✓	✓
$p_{\mathrm{T}}^{\mathrm{miss,proj}}$	✓	
$p_{\mathrm{T}}^{\ell\ell}$	✓	✓
$m_{\ell\ell}$	✓	
$m_{\ell\ell\,p_{\mathrm{T}}^{\mathrm{miss}}}$	✓	
$\Delta\phi_{\ell\ell\,p_{\mathrm{T}}^{\mathrm{miss}}}$	✓	✓
$\Delta\phi_{\ell\mathrm{J}}$		✓
$\Delta\phi_{p_{\mathrm{T}}^{\mathrm{miss}}\mathrm{J}}$		✓
$\Delta\phi_{\ell\ell}$	✓	
H_{T}		✓
Recoil	✓	✓

on the basis of scores: $S_{\mathrm{DY}} > 0.6$ and $S_{t\bar{t}} < 0.6$. Many kinematic distributions are examined and all show good agreement between simulation and data in this control region. This control region is used to set the normalization of the top quark background in the signal region.

The next largest background contribution comes from the Drell-Yan process, which is larger in the SF channel than in the DF channel. The nature of these contributions is somewhat different. The SF contribution arises mainly from the portion of Drell-Yan production that falls below or above the Z resonance peak. The sequential analysis calibrates this contribution using the observed number of events in the Z peak and the ratio of numbers of events inside and outside the peak, as estimated from simulations. The DF contribution arises from $Z \to \tau^+\tau^-$ production with both τ leptons decaying leptonically. The sequential cut analysis verifies the $Z \to \tau^+\tau^-$ background using a control region defined by $m_{e\mu} < 80$ GeV and inverted $p_{\mathrm{T}}^{\ell\ell}$ requirements. The random forest analysis defines a Drell-Yan control region by $S_{\mathrm{DY}} < 0.6$ and $S_{t\bar{t}} > 0.6$, which includes both SF and DF events. Simulations of kinematic distributions for events in this region match the data well, and the yield of events in this region is used to normalize the Drell-Yan background contribution in the signal region.

The next most important background contribution comes mainly from W boson events in which a nonprompt lepton from a jet is selected in addition to a lepton from the W boson decay. Monte Carlo simulation cannot be used for an accurate estimate of this contribution, but it can be used to devise and evaluate an estimate based on control samples. In the sequential cut analysis, a "pass-fail" control sample is defined by one lepton that passes the lepton selection criteria and another that fails the criteria but passes looser criteria. The misidentification rate f for a jet that satisfies loose lepton requirements to also pass the standard lepton requirements is determined using an event sample dominated by multijet events with nonprompt leptons. This misidentification rate is parametrized as a function of lepton p_{T} and η and used to compute weights $f/(1-f)$ in the pass-fail sample that are used to determine the contribution of nonprompt leptons in the signal region [46,47]. The random forest analysis uses a different method based on a control region in which the two leptons have the same charge. This control region is dominated by $W + \text{jets}$ events with contributions from diboson and other events. The transfer factor relating the number of same-sign events in the control region to the number of opposite-sign events in the signal region is based on two methods relying on data control samples and which are validated using simulations. One method uses events with DF leptons and low $p_{\mathrm{T}}^{\mathrm{miss}}$ and the other uses events with an inverted isolation requirement. Both methods yield values for the transfer factor that are consistent at the 16% level.

Background contamination from $W\gamma^*$ events with low-mass $\gamma^* \to \ell^+\ell^-$ can satisfy the signal event selection

when the transverse momenta of the two leptons are very different [46]. The predicted contribution in the signal region is normalized to the number of events in a control region with three muons satisfying $p_T > 10$, 5, and 3 GeV and for $m_{\gamma^*} < 4$ GeV. In this control region, the requirement $p_T^{\text{miss}} < 25$ GeV is imposed in order to suppress non-$W\gamma^*$ events.

The remaining minor sources of background, including diboson and triboson final states and Higgs-mediated W^+W^- production, are evaluated using simulations normalized to the most precise theoretical cross sections available.

VII. SIGNAL EXTRACTION

The cross sections are obtained by simultaneously fitting the predicted yields to the observed yields in the signal and control regions. In this fit, a signal strength parameter modifies the predicted signal yield defined by the central value of the theoretical cross section, $\sigma_{\text{tot}}^{\text{NNLO}} = 118.8 \pm 3.6$ pb. The fitted value of the signal strength is expected to be close to unity if the SM is valid, and the measured cross section is the product of the signal strength and the theoretical cross section. Information from control regions is incorporated in the analysis through additional parameters that are free in the fit; the predicted background in the signal region is thereby tied to the yields in the control regions. In the sequential cut analysis, there is one control region enriched in $t\bar{t}$ events; the yields in the signal and this one control region are fit simultaneously. Since the selected event sample is separated according to SF and DF, 0- and 1-jet selections, there are eight fitted yields. In the random forest analysis, there are three control regions, one for Drell-Yan background, a second for $t\bar{t}$ background, and a third for events with nonprompt leptons (e.g., W + jets). Since SF and DF final states are analyzed together, and the selection does not explicitly distinguish the number of jets, there are four fitted yields in the random forest analysis. In both analyses, the yields in the control regions effectively constrain the predicted backgrounds in the signal regions.

Additional nuisance parameters are introduced in the fit that encapsulate important sources of systematic uncertainty, including the electron and muon efficiencies, b-tagging efficiencies, the jet energy scale, and the predicted individual contributions to the background. The total signal strength uncertainty, including all systematic uncertainties, is determined by the fit with all parameters free; the statistical uncertainty is determined by fixing all parameters except the signal strength to their optimal values.

VIII. SYSTEMATIC UNCERTAINTIES

Experimental and theoretical sources of systematic uncertainty are described in this section. A summary of all systematic uncertainties for the cross section measurement is given in Table IV. These sources of uncertainty

TABLE IV. Relative systematic uncertainties in the total cross section measurement (0- and 1-jet, DF, and SF) based on the sequential cut analysis.

Uncertainty source	(%)
Statistical	1.2
$t\bar{t}$ normalization	2.0
Drell-Yan normalization	1.4
$W\gamma^*$ normalization	0.4
Nonprompt leptons normalization	1.9
Lepton efficiencies	2.1
b tagging (b/c)	0.4
Mistag rate (q/q)	1.0
Jet energy scale and resolution	2.3
Pileup	0.4
Simulation and data control regions sample size	1.0
Total experimental systematic	4.6
QCD factorization and renormalization scales	0.4
Higher-order QCD corrections and p_T^{WW} distribution	1.4
PDF and α_S	0.4
Underlying event modeling	0.5
Total theoretical systematic	1.6
Integrated luminosity	2.7
Total	5.7

impact the measurements of the cross section through the normalization of the signal. Many of them also impact kinematic distributions that ultimately can alter the shapes of distributions studied in this analysis. Both normalization and shape uncertainties are evaluated.

A. Experimental sources of uncertainty

There are several sources of experimental systematic uncertainties, including the lepton efficiencies, the b-tagging efficiency for b quark jets and the mistag rate for light-flavor quark and gluon jets, the lepton momentum and energy scales, the jet energy scale and resolution, the modeling of p_T^{miss} and of pileup in the simulation, the background contributions, and the integrated luminosity.

The sequential cut and the random forest analyses both use control regions to estimate the background contributions in the signal region. The uncertainties in the estimates are determined mainly by the statistical power of the control regions, though the uncertainty of the theoretical cross sections and the shape of the Z resonant peak also play a role. Sources of systematic uncertainty of the estimated Drell-Yan background include the Z resonance line shape and the performance of the DYMVA classifier for different p_T^{miss} thresholds. These uncertainties are propagated directly to the predicted SF and DF background estimates. The contribution from nonprompt leptons is entirely determined by the methods based on data control regions, described in Sec. VI; typically these contributions are uncertain at approximately the 30% level. The contribution from the $W\gamma^*$ final state is checked using a sample

of events with three well-identified leptons including a low-mass, opposite-sign pair of muons. The comparison of the MC prediction with the data has an uncertainty of about 20%. The other backgrounds are estimated using simulations and their uncertainties depend on the uncertainties of the theoretical cross sections, which are typically below 10%. Statistical uncertainties from the limited number of MC events are taken into account and have a very small impact on the result.

Small differences in the lepton trigger, reconstruction, and identification efficiencies for data and simulation are corrected by applying scale factors to adjust the efficiencies in the simulation. These scale factors are obtained using events in the Z resonance peak region [42,43] recorded with unbiased triggers. They vary with lepton p_T and η and are within 3% of unity. The uncertainties of these scale factors are mostly at the 1%–2% level.

Differences in the probabilities for b jets and light-flavor quark and gluon jets to be tagged by the CSV v2 algorithm are corrected by applying scale factors to the simulation. These scale factors are measured using $t\bar{t}$ events with two leptons [40]. These scale factors are uncertain at the percent level and have relatively little impact on the result because the signal includes mainly light-flavor quark and gluon jets, which have a low probability to be tagged, and the top quark background is assessed using appropriate control regions.

The jet energy scale is set using a variety of *in situ* calibration techniques [48]. The remaining uncertainty is assessed as a function of jet p_T and η. The jet energy resolution in simulated events is slightly different than that measured in data. The differences between simulation and data lead to uncertainties in the efficiency of the event selection because the number of selected jets, their transverse momenta, and also p_T^{miss} play a role in the event selection.

The lepton energy scales are set using the position of the Z resonance peak; the uncertainties are very small and have a negligible impact on the measurements reported here.

The modeling of pileup depends on the total inelastic pp cross section [49]. The pileup uncertainty is evaluated by varying this cross section up and down by 5%.

The statistical uncertainties from the limited number of events in the various control regions lead to a systematic uncertainty from the background predictions. It is listed as part of the experimental systematic uncertainty in Table IV.

The uncertainty in the integrated luminosity measurement is 2.5% [50]. It contributes directly to the cross section and also to the uncertainty in the minor backgrounds predicted from simulation.

B. Theoretical sources of uncertainty

The efficiency of the event selection is sensitive to the number of hadronic jets in the event. The sequential cut analysis explicitly singles out events with zero or one jet,

and the random forest classifiers utilize quantities, such as H_T, that tend to correlate with the number of jets. As a consequence, the efficiency of the event selection is sensitive to higher-order QCD corrections that are adequately described by neither the matrix-element calculation of POWHEG nor by the parton shower simulation. The uncertainty reflecting these missing higher orders is evaluated by varying the QCD factorization and renormalization scales independently up and down by a factor of 2 but excluding cases in which one is increased and the other decreased simultaneously. A change in measured cross sections is evaluated by applying appropriate weights to the simulated events.

Some of the higher-order QCD contributions to W^+W^- production have been calculated using the p_T-resummation [51,52] and the jet-veto resummation [53] techniques. The results from these two approaches are compatible [54]. The transverse momentum p_T^{WW} of the W^+W^- pair is used as a proxy for these higher-order corrections; the p_T^{WW} spectrum from POWHEG is reweighted to match the analytical prediction obtained using the p_T-resummation at next-to-next-to-leading logarithmic accuracy [51]. Uncertainties in the theoretical calculation of the p_T^{WW} spectrum lead to uncertainties in the event selection efficiency that are assessed for the $qq \rightarrow W^+W^-$ process by independently varying the resummation, the factorization, and the renormalization scales in the analytical calculation [52]. The uncertainty in the $gg \rightarrow W^+W^-$ component is determined by the variation of the renormalization and factorization scales in the theoretical calculation of this process [9].

Additional sources of theoretical uncertainties come from the PDFs and the assumed value of α_S. The PDF uncertainties are estimated, following the PDF4LHC recommendations [55], from the variance of the values obtained using the set of MC replicas of the NNPDF3.0 PDF set. The variation of both the signal and the backgrounds with each PDF set and the value of α_S is taken into account.

The uncertainty from the modeling of the underlying event is estimated by comparing the signal efficiency obtained with the $qq \rightarrow W^+W^-$ sample described in Sec. III to alternative samples that use different generator configurations.

The branching fraction for leptonic decays of W bosons is taken to be $\mathcal{B}(W \rightarrow \ell\nu) = 0.1086 \pm 0.0009$ [56], and lepton universality is assumed to hold. The uncertainty coming from this branching fraction is not included in the total uncertainty; it would amount to 1.8% of the cross section value.

IX. THE W^+W^- CROSS SECTION MEASUREMENTS

Two measurements of the total production cross section are reported in this section: the primary one coming from the sequential cut analysis and a secondary measurement

TABLE V. Summary of the signal strength and total production cross section obtained in the sequential cut analysis. The uncertainty listed is the total uncertainty obtained from the fit to the yields.

Category		Signal strength	Cross section [pb]
0-jet	DF	1.054 ± 0.083	125.2 ± 9.9
0-jet	SF	1.01 ± 0.16	120 ± 19
1-jet	DF	0.93 ± 0.12	110 ± 15
1-jet	SF	0.76 ± 0.20	89 ± 24
0-jet and 1-jet	DF	1.027 ± 0.071	122.0 ± 8.4
0-jet and 1-jet	SF	0.89 ± 0.16	106 ± 19
0-jet and 1-jet	DF and SF	0.990 ± 0.057	117.6 ± 6.8

coming from the random forest analysis. In addition, measurements of the fiducial cross section are reported, based on the sequential cut analysis, including the change of the zero-jet cross section with variations of the jet p_T threshold.

A. Total production cross section

Both the sequential cut and random forest analyses provide precise measurements of the total production cross section. Since the techniques for selecting signal events are rather different, both values are reported here. The measurement obtained with the sequential cut analysis is the primary measurement of the total production cross section, because it is relatively insensitive to the uncertainties in the corrections applied to the p_T^{WW} spectrum. The overlap of the two sets of selected events is approximately 50%. A combination of the two measurements is not carried out because the reduction in the uncertainty would be minor.

The sequential cut (SC) analysis makes a double dichotomy of the data: selected events are separated if the leptons are DF or SF (DF is purer because of a smaller Drell-Yan contamination), and these are further subdivided depending on whether there is zero or one jet (0-jet is purer because of a smaller top quark contamination). The comparison of the four signal strengths provides an important test of the consistency of the measurement; the cross section value is based on the simultaneous fit of DF and SF and 0-jet and 1-jet channels. The result is $\sigma_{SC}^{tot} = 117.6 \pm 1.4(\text{stat}) \pm 5.5(\text{syst}) \pm 1.9(\text{theo}) \pm 3.2(\text{lumi})$ pb $= 117.6 \pm 6.8$ pb, which is consistent with the theoretical prediction $\sigma_{tot}^{NNLO} = 118.8 \pm 3.6$ pb. A summary of the measured signal strengths and the corresponding cross sections is given in Table V.

The random forest analysis isolates a purer signal than the sequential cut analysis (see Table II); however, its sensitivity is concentrated at relatively low p_T^{WW} as shown in Fig. 4. This region corresponds mainly to events with zero jets; the random forest classifier uses observables such as H_T that correlate with jet multiplicity and reduce top quark background contamination by favoring events with a
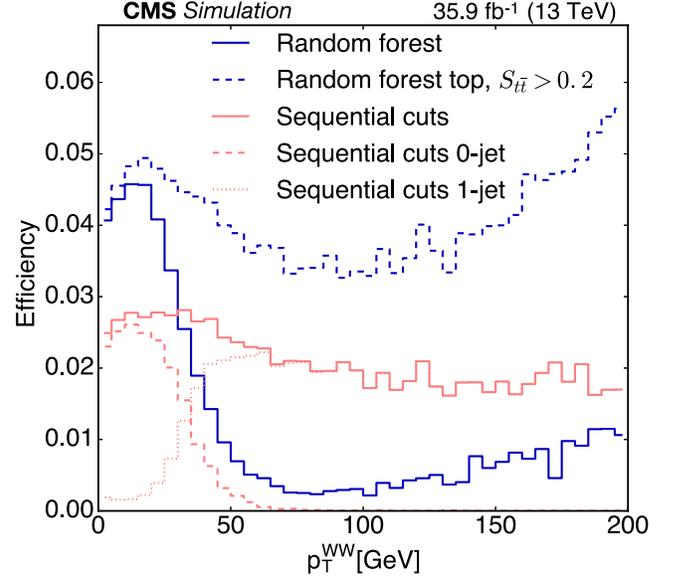

FIG. 4. Comparison of efficiencies for the sequential cut and random forest analyses as a function of p_T^{WW}. The sequential cut analysis includes 0- and 1-jet events from both DF and SF lepton combinations, for which the contributions from 0- and 1-jet are shown separately. The efficiency curve for $S_{t\bar{t}}^{min} = 0.2$ is also shown; this value is used in measuring the jet multiplicity distribution.

low jet multiplicity. As a consequence, the random forest result is more sensitive to uncertainties in the theoretical corrections to the p_T^{WW} spectrum than the sequential cut analysis. The signal strength measured by the random forest analysis is 1.106 ± 0.073 which corresponds to a measured total production cross section of $\sigma_{RF}^{tot} = 131.4 \pm 1.3(\text{stat}) \pm 6.0(\text{syst}) \pm 5.1(\text{theo}) \pm 3.5(\text{lumi})$ pb $= 131.4 \pm 8.7$ pb. The difference with respect to the sequential cut analysis reflects the sensitivity of the random forest analysis to low p_T^{WW}.

B. Fiducial cross sections

The sequential cut analysis is used to obtain fiducial cross sections. The definition of the fiducial region is similar to the requirements described in Sec. VA above. The generated event record must contain two prompt leptons (electrons or muons) with $p_T > 20$ GeV and $|\eta| < 2.5$. Decay products of τ leptons are not considered part of the signal in this definition of the fiducial region. Other kinematic requirements are applied: $m_{\ell\ell} > 20$ GeV, $p_T^{\ell\ell} > 30$ GeV, and $p_T^{miss} > 20$ GeV (where p_T^{miss} is calculated using the momenta of the neutrinos emitted in the W boson decays). When categorizing events with zero or more jets, a jet is defined using stable particles but not neutrinos. For the baseline measurements, the jets must have $p_T > 30$ GeV and $|\eta| < 4.5$ and be separated from each of the two leptons by $\Delta R > 0.4$.

TABLE VI. Fiducial cross section for the production of $W^+W^- + 0$-jets as the p_T threshold for jets is varied. The fiducial region is defined by two opposite-sign leptons with $p_T >$ 20 GeV and $|\eta| < 2.5$ excluding the products of τ lepton decay, and $m_{\ell\ell} > 20$ GeV, $p_T^{\ell\ell} > 30$ GeV, and $p_T^{\text{miss}} > 30$ GeV. Jets must have p_T above the stated threshold, $|\eta| < 4.5$, and be separated from each of the two leptons by $\Delta R > 0.4$. The total uncertainty is reported.

p_T threshold (GeV)	Signal strength	Cross section (pb)
25	1.091 ± 0.073	0.836 ± 0.056
30	1.054 ± 0.065	0.892 ± 0.055
35	1.020 ± 0.060	0.932 ± 0.055
45	0.993 ± 0.057	1.011 ± 0.058
60	0.985 ± 0.059	1.118 ± 0.067

The fiducial cross section is obtained by means of a simultaneous fit to the DF and SF, 0- and 1-jet final states. The measured value is $\sigma^{\text{fid}} = 1.529 \pm 0.020(\text{stat}) \pm 0.069(\text{syst}) \pm 0.028(\text{theo}) \pm 0.041(\text{lumi})$ pb $= 1.529 \pm 0.087$ pb, which agrees well with the theoretical value $\sigma_{\text{NNLO}}^{\text{fid}} = 1.531 \pm 0.043$ pb. These values are corrected to the fiducial region with all jet multiplicities.
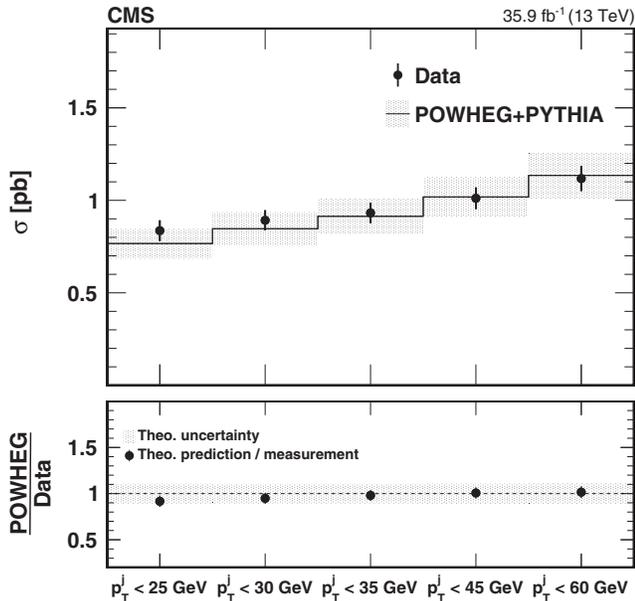

FIG. 5. The upper panel shows the fiducial cross sections for the production of $W^+W^- + 0$-jets as the p_T threshold for jets is varied. The fiducial region is defined by two opposite-sign leptons with $p_T > 20$ GeV and $|\eta| < 2.5$ excluding the products of τ lepton decay, and $m_{\ell\ell} > 20$ GeV, $p_T^{\ell\ell} > 30$ GeV, and $p_T^{\text{miss}} > 30$ GeV. Jets must have p_T above the stated threshold, $|\eta| < 4.5$, and be separated from each of the two leptons by $\Delta R > 0.4$. The lower panel shows the ratio of the theoretical prediction to the measurement. In both the upper and lower panels, the error bars on the data points represent the total uncertainty of the measurement, and the shaded band depicts the uncertainty of the MC prediction.

The fiducial cross sections for the production of W^+W^- boson pairs with zero or one jet are of interest because some of the earlier measurements were based on the 0-jet subset only, i.e., a jet veto was applied [2–4,6]. The sequential cut analysis provides the following values based on the combination of the DF and SF categories: $\sigma^{\text{fid}}(0\text{-jet}) = 1.61 \pm 0.10$ pb and $\sigma^{\text{fid}}(1\text{-jet}) = 1.35 \pm 0.11$ pb for a jet p_T threshold of 30 GeV. These fiducial cross section values pertain to the definition given above; in particular, they pertain to all jet multiplicities.

The fiducial cross section for $W^+W^- + 0$-jets production is also measured as a function of the jet p_T threshold in the range 25–60 GeV with the results listed in Table VI and displayed in Fig. 5. The cross section is expected to increase with jet p_T threshold because the phase space for zero jets increases.

X. NORMALIZED DIFFERENTIAL CROSS SECTION MEASUREMENTS

Differential cross sections are measured for the fiducial region defined above using the sequential cut, DF event selection. The random forest selection is unsuitable for measuring these differential cross sections because some of these kinematic quantities are used as inputs to the random forest classifiers. These differential cross sections are normalized to the measured integrated fiducial cross section, which for the DF final state (0- and 1-jet) is 0.782 ± 0.053 pb corresponding to a signal strength of 1.022 ± 0.069.

For each differential cross section, a simultaneous fit to the reconstructed distribution is performed in the following manner. An independent signal strength parameter is assigned to each generator-level histogram bin. For the MC simulated events falling within a given generator-level bin, a template histogram of the reconstructed kinematic quantity is formed. The detector resolution is good for the quantities considered, so the template histogram has a peak corresponding to the given generator-level bin; the contents of all bins below and above the given generator-level bin are relatively low. When the fit is performed, the signal strengths are allowed to vary independently. The correlations among bins in the distribution of the reconstructed quantity are taken into account. The fitted values of the signal strength parameters are applied to the generator-level differential cross section to obtain the measured differential cross section.

Measurements of the differential cross sections with respect to the dilepton mass $(1/\sigma)d\sigma/dm_{\ell\ell}$, the leading lepton transverse momentum $(1/\sigma)d\sigma/dp_T^{\ell\,\text{max}}$, the trailing lepton transverse momentum $(1/\sigma)d\sigma/dp_T^{\ell\,\text{min}}$, and the angular separation between the leptons $(1/\sigma)d\sigma/d\Delta\phi_{\ell\ell}$ are reported. The measurements are compared to simulations generated with POWHEG+PYTHIA in Fig. 6.
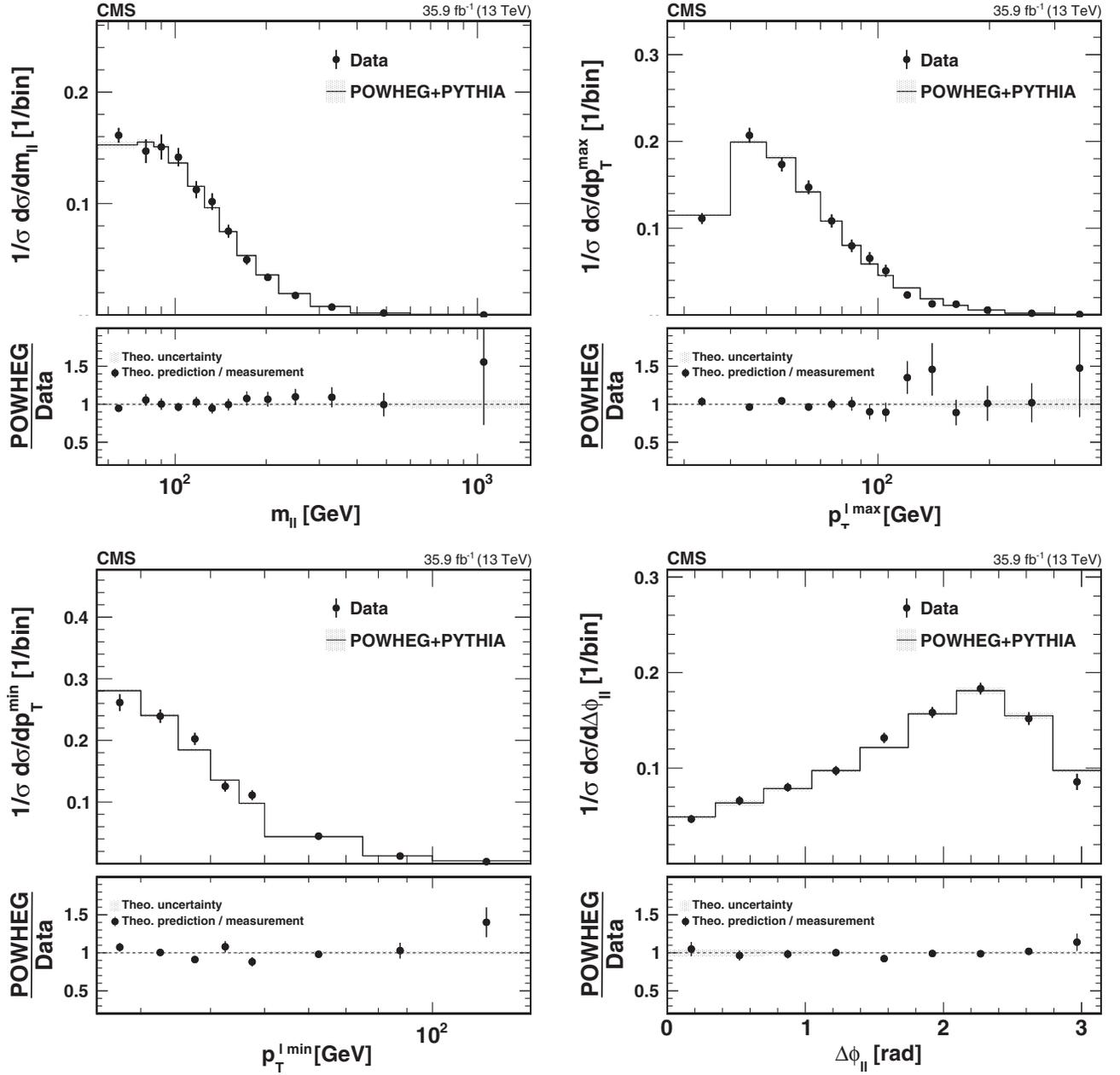
FIG. 6.   The upper panels show the normalized differential cross sections with respect to the dilepton mass $m_{\ell\ell}$, leading lepton $p_T^{\ell\,\mathrm{max}}$, trailing lepton $p_T^{\ell\,\mathrm{min}}$, and dilepton azimuthal angular separation $\Delta\phi_{\ell\ell}$, compared to POWHEG predictions. The lower panels show the ratio of the theoretical predictions to the measured values. The meaning of the error bars and the shaded bands is the same as in Fig. 5.

XI. JET MULTIPLICITY MEASUREMENT

A measurement of the jet multiplicity tests the accuracy of theoretical calculations and event generators. Signal W^+W^- events are characterized by a low jet multiplicity in contrast to $t\bar{t}$ background events, which typically have two or three jets. The sequential event selection exploits this difference by eliminating events with more than one jet and by separating 0- and 1-jet event categories. The random forest selection, in contrast, places no explicit requirements on the number of jets (N_J) in an event, and the separation of

signal W^+W^- events and $t\bar{t}$ background utilizes other event features listed in Table III. As a consequence, a precise measurement of the fractions of events with $N_J = 0$, 1, or ≥ 2 jets can be made. For this measurement, jets have $p_T > 30$ GeV and $|\eta| < 2.4$, and must be separated from each of the selected leptons by $\Delta R > 0.4$. The rejection of events with one or more b-tagged jets is still in effect; however, the impact on the signal is very small.

The anti-$t\bar{t}$ random forest produces a continuous score, $S_{t\bar{t}}$, in the range $0 \leq S_{t\bar{t}} \leq 1$, as explained in Sec. V B.

TABLE VII. Efficiency for the random forest selection with respect to preselected events as a function of jet multiplicity. The stated uncertainties are statistical only.

Number of jets	0	1	≥ 2
Efficiency	0.555 ± 0.003	0.448 ± 0.004	0.290 ± 0.004

For the measurement of the jet multiplicity presented in this section, the criterion against $t\bar{t}$ background is loosened to $S_{t\bar{t}}^{\min} = 0.2$ while $S_{\mathrm{DY}}^{\min} = 0.96$ remains. This looser requirement leads to a signal efficiency for the random forest selection with a relatively gentle variation with N_{J} as shown in Table VII, and also a more even variation of the efficiency as a function of p_{T}^{WW}, as shown in Fig. 4. These efficiencies are defined for the events passing the random forest selection with respect to those passing the preselection requirements. The efficiency for the preselection is essentially independent of N_{J}.

Background contributions are subtracted from the observed numbers of events as a function of N_{J} and then corrections are applied for the random forest efficiencies shown in Table VII. The observed jet multiplicity suffers from the migration of events from one N_{J} bin to another due to two experimental effects: first, pileup can produce extra jets (pileup), and second, jet energy mismeasurements can lead to jets with true p_{T} below the 30 GeV threshold being accepted and others with true p_{T} above 30 GeV being rejected. Pileup jets only increase the number of jets in an event, while energy calibration and resolution lead to both increase and decrease in N_{J}. Because of the falling jet p_{T} distribution, the jet energy resolution leads to increases in N_{J} more often than to decreases.

The two sources of event migration are corrected in two distinct steps. The signal MC event sample is used to build two response matrices: $\mathbf{R}_{\mathrm{PU}}$ for pileup and $\mathbf{R}_{\mathrm{det}}$ for detector effects, in particular, jet energy resolution. The reconstructed jet multiplicity for the signal process is given by $\vec{v} = \mathbf{R}_{\mathrm{PU}} \mathbf{R}_{\mathrm{det}} \vec{t}$, where $\vec{v}$ and $\vec{t}$ are vectors representing the multiplicity distribution; $\vec{t}$ represents the MC "truth" as inferred from generator-level jets and $\vec{v}$ is the reconstructed distribution. Generator-level jets are reconstructed from generated stable particles, excluding neutrinos, with the clustering algorithm used to reconstruct jets in data. These jets must satisfy $p_{\mathrm{T}} > 30$ GeV and $|\eta| < 2.4$ and must be separated by $\Delta R > 0.4$ from both of the two leptons from

W boson decays. Reconstructed and generator-level jets are said to match if they have $\Delta R < 0.4$. On the basis of the simulated signal event sample, the two response matrices are close to being diagonal,

$$\mathbf{R}_{\mathrm{PU}} = \begin{pmatrix} 0.986 & 0 & 0 \\ 0.013 & 0.985 & 0 \\ 0.001 & 0.015 & 1 \end{pmatrix}$$

$$\mathbf{R}_{\mathrm{det}} = \begin{pmatrix} 0.963 & 0.060 & 0.003 \\ 0.036 & 0.891 & 0.090 \\ 0.001 & 0.049 & 0.906 \end{pmatrix}.$$

Here, the columns correspond to $N_{\mathrm{J}} = 0$, 1, ≥ 2 for generator-level jets, and the rows to the same for reconstructed jets.

The response matrices are used to unfold the distribution of jet multiplicities according to $\vec{u} = \mathbf{R}_{\mathrm{DET}}^{-1} \mathbf{R}_{\mathrm{PU}}^{-1} \vec{v}$. No regularization procedure is applied. The fractions of events with $N_{\mathrm{J}} = 0$, 1, ≥ 2 jets are obtained by normalizing $\vec{u}$ to unit norm: the unfolded result is $\vec{w} = \vec{u}/|\vec{u}|$.

All systematic uncertainties are reevaluated for the jet multiplicity measurement. Since the observables are essentially yields normalized to the total number of events, systematic uncertainties from the integrated luminosity and lepton efficiency are negligible. The statistical uncertainty in the response matrix is also negligible. Non-negligible uncertainties are obtained for the jet energy scale and resolution, for pileup reweighting, and for reweighting of the p_{T}^{WW} spectrum. The total relative uncertainties for the elements of the response matrix are

$$\begin{pmatrix} 0.011 & 0.193 & 0.374 \\ 0.210 & 0.007 & 0.140 \\ 0.305 & 0.181 & 0.015 \end{pmatrix}.$$

Although the relative uncertainty of the off-diagonal matrix elements is large, those elements themselves are small, so a precise measurement is still achievable.

Table VIII reports the measured fractions of events with N_{J} jets. The fractions before unfolding for pileup and jet energy resolution are listed, as well as the prediction based on POWHEG weighted to correct the W^+W^- p_{T} spectrum. Figure 7 shows a comparison of the measured fractions and

TABLE VIII. Fractions of events with $N_{\mathrm{J}} = 0$, 1, ≥ 2 jets. The first uncertainty is statistical, and the second combines systematic uncertainties from the response matrix and from the background subtraction.

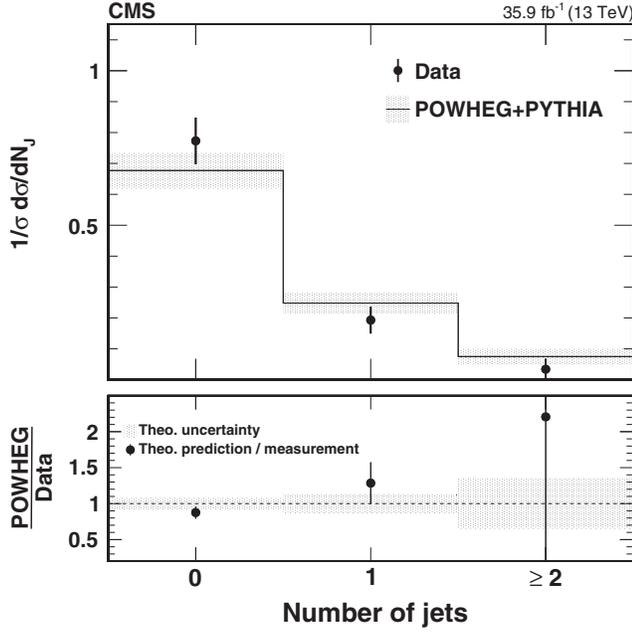| Number of jets	0	1	≥ 2
Before unfolding	$0.795 \pm 0.007 \pm 0.053$	$0.180 \pm 0.006 \pm 0.039$	$0.025 \pm 0.005 \pm 0.018$
After unfolding	$0.773 \pm 0.008 \pm 0.075$	$0.193 \pm 0.007 \pm 0.043$	$0.034 \pm 0.006 \pm 0.033$
Predicted	$0.677 \pm 0.007 \pm 0.058$	$0.248 \pm 0.007 \pm 0.033$	$0.075 \pm 0.006 \pm 0.026$

FIG. 7. The upper panel shows the fractions of events with $N_J = 0, 1, \geq 2$ jets. The filled circles represent the data after backgrounds are subtracted and pileup and energy resolution are taken into account. The solid lines represent the POWHEG+PYTHIA prediction. The lower panel shows the ratio of the theoretical prediction to the measurement. The meaning of the error bars and the shaded bands is the same as in Fig. 5.

the prediction from POWHEG. For this prediction, the p_T^{WW} spectrum is reweighted as described in Sec. VIII B.

XII. LIMITS ON DIMENSION-6 WILSON COEFFICIENTS

In the framework of effective field theory, new physics can be described in terms of an infinite series of new interaction terms organized as an expansion in the mass dimension of the corresponding operators [57]. The dimension-4 operators of the SM comprise the zeroth term of the expansion. The series can be understood as coming from the integration of heavy fields in an ultraviolet-complete theory, which itself is renormalizable and unitary. When testing for the presence of these higher-dimensional operators, it is assumed that just one or two operators have non-vanishing coefficients in order to reduce the computational burden. A truncated series, for example, a series including the SM and dimension-6 operators only, is not renormalizable and will violate tree-level unitarity at some energy scale. Consequently, the truncated series is useful only when the scale of new physics is large compared to the energies accessible in the given final state, in which case terms including higher-dimensional operators are suppressed.

In the electroweak sector of the SM, the first higher-dimensional operators containing only massive boson fields are dimension-6 [15,58],

$$\mathcal{O}_{WWW} = \frac{c_{WWW}}{\Lambda^2} W_{\mu\nu} W^{\nu\rho} W_\rho{}^\mu$$

$$\mathcal{O}_W = \frac{c_W}{\Lambda^2} (D^\mu \Phi)^\dagger W_{\mu\nu} (D^\nu \Phi)$$

$$\mathcal{O}_B = \frac{c_B}{\Lambda^2} (D^\mu \Phi)^\dagger B_{\mu\nu} (D^\nu \Phi)$$

$$\tilde{\mathcal{O}}_{WWW} = \frac{\tilde{c}_{WWW}}{\Lambda^2} \tilde{W}_{\mu\nu} W^{\nu\rho} W_\rho{}^\mu$$

$$\tilde{\mathcal{O}}_W = \frac{\tilde{c}_W}{\Lambda^2} (D^\mu \Phi)^\dagger \tilde{W}_{\mu\nu} (D^\nu \Phi).$$

The gauge group indices are suppressed for clarity and the mass scale Λ has been factored out from the Wilson coefficients c and $\tilde{c}$. The tensor $W_{\mu\nu}$ is the $SU(2)$ field strength, $B_{\mu\nu}$ is the $U(1)$ field strength, Φ is the Higgs doublet, and operators with a tilde are the magnetic duals of the field strengths. The first three operators are CP conserving, while the last two are not. In this analysis, only the CP conserving operators are considered.

These operators contribute to several multiboson scattering processes at tree level. The operator $\mathcal{O}_{WWW}$ modifies vertices with three to six vector bosons, while $\mathcal{O}_W$ and $\mathcal{O}_B$ modify both HVV vertices and vertices with three or four vector bosons. The focus in this analysis is on modifications to the vertices HW^+W^-, γW^+W^-, and ZW^+W^- since they lead to deviations of the $pp \to W^+W^-$ cross section via diagrams of the kind shown in Fig. 8.

The analysis is based on the DF event sample selected in the sequential cut analysis. The SF event sample is not used because the contamination from Drell-Yan processes is larger and the selected event sample itself is smaller. The 0- and 1-jet categories are analyzed separately. The signal region and the top quark control region are both included in the analysis.

The invariant mass $m_{e\mu}$ distribution is used to test for dimension-6 operators. The quantity $m_{e\mu}$ is well measured and is not sensitive to higher-order QCD effects and jet energy calibration issues. Furthermore, the $m_{e\mu}$ distribution is more sensitive to higher-dimensional operators than other observables based on lepton kinematics. In order to suppress the Higgs boson contribution and enhance the sensitivity to higher-dimensional operators, the requirement $m_{e\mu} > 100$ GeV is imposed. The remaining Higgs boson contributions are considered part of the signal.
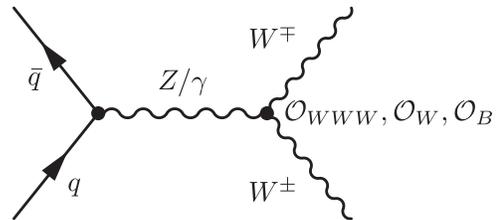

FIG. 8. One of the Feynman diagrams through which dimension-6 operators modify the $pp \to W^+W^-$ cross section.
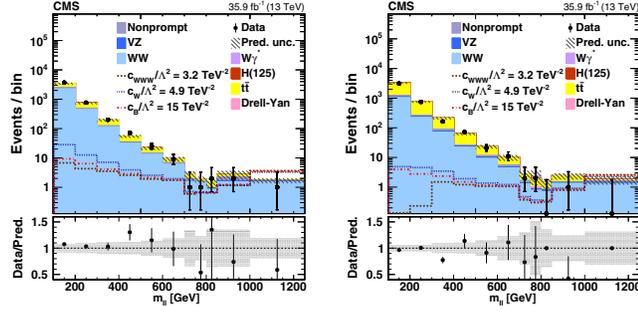
FIG. 9. Comparison of the template fits to the observed $m_{e\mu}$ distributions in the 0-jet (left) and 1-jet (right) categories. The non-SM contributions for $c_{WWW}/\Lambda^2 = 3.2$ TeV^{-2}, $c_W/\Lambda^2 = 4.9$ TeV^{-2}, and $c_B/\Lambda^2 = 15.0$ TeV^{-2} are shown, not stacked on top of the other contributions. In the plot on the right, the decrease in the non-SM contribution at low $m_{e\mu}$ is not statistically significant and results from limited precision in the subtraction of two large yields (SM and SM + non-SM). The last bin contains all events with reconstructed $m_{e\mu} > 1$ TeV. The error bars on the data points represent the statistical uncertainties for the data, and the hatched areas represent the total uncertainty for the predicted yield in each bin.

Variations of the relatively small VZ background processes due to dimension-6 operators are neglected.

The measurement of the Wilson coefficients uses templates of $m_{e\mu}$ with the following bins: [100, 200, 300, 400, 500, 600, 700, 750, 800, 850, 1000, ∞] GeV; the last bin contains all events with $m_{e\mu} > 1$ TeV. This choice minimizes the expected 95% confidence level (C.L.) intervals for all coefficients (with fixed mass scale Λ) while populating each bin adequately. The highest bin is the one with the greatest statistical power largely because of the presence of multiple momentum factors in the Feynman diagrams associated with the higher-dimensional operators (Fig. 8).

In order to construct the $m_{e\mu}$ templates, the weights calculated for each event are used to build a parametrized model of the expected yield in each bin as a function of the coefficients (with fixed Λ). More precisely, for each bin, a fit is performed of a second-order polynomial to the ratios of the expected signal yield with nonzero coefficients to the one without (SM). When only one coefficient is taken to be nonzero, the fit is performed to five points, and when two coefficients are taken to be nonzero, the fit is performed to a 5×5 grid. These fits are carried out for the 0- and 1-jet categories separately.

A binned maximum likelihood fit of the $m_{e\mu}$ templates to the data is carried out. The likelihood is computed using the Poisson probability for each bin i with $N_i^{\exp}$ expected events and N_i^{obs} observed events. Each source of uncertainty is modeled with a log-normal distribution $\pi_{ij}(\theta_j)$ where θ_j is the nuisance parameter for a source of uncertainty j as discussed in Sec. VIII. The expected yields $N_i^{\exp}$ are

functions of the nuisance parameters θ_j. The likelihood is computed from the product over all bins i,

$$L = \prod_{i=i}^{N} \left[e^{-N_i^{\exp}} (N_i^{\exp})^{N_i^{\mathrm{obs}}} \prod_{j=i}^{M} \pi_{ij}(\theta_j) \right],$$

where the $N!$ term has been neglected. The nuisance parameters for the systematic uncertainties are profiled for each dimension-6 operators hypothesis.

Figure 9 shows the results of the template fits to the observed $m_{e\mu}$ distributions. The expected signal distributions for three values of the coefficients close to the 95% C.L. expected limits on those coefficients are also shown (not stacked); the largest impact of nonzero coefficients is seen for $m_{e\mu} > 850$ GeV.

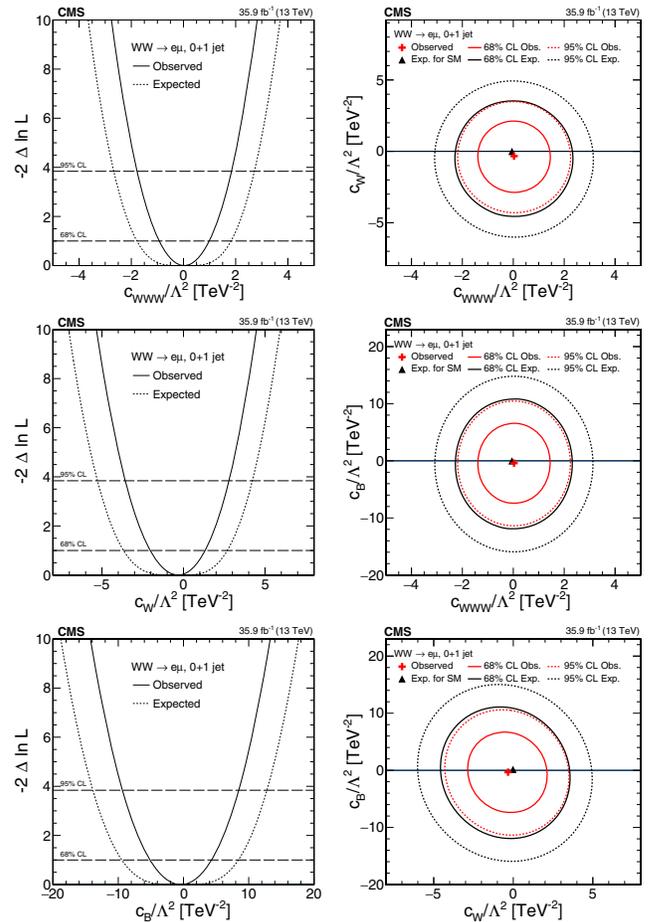Figure 10 (left) shows the curves of $-2\Delta \ln L = -2(\ln L - \ln L_{\min})$ for the three dimension-6 operators

FIG. 10. On the left, the expected and observed $-2\Delta \ln L$ curves for the c_{WWW}/Λ^2, c_W/Λ^2, and c_B/Λ^2 combining the 0- and 1-jet categories. On the right, the expected and observed 68% and 95% confidence level contours in the $(c_{WWW}/\Lambda^2, c_W/\Lambda^2)$, $(c_{WWW}/\Lambda^2, c_B/\Lambda^2)$, and $(c_W/\Lambda^2, c_B/\Lambda^2)$ planes combining the 0- and 1-jet categories.

TABLE IX.   Expected and observed 68% and 95% confidence intervals on the measurement of the Wilson coefficients associated with the three *CP*-conserving, dimension-6 operators.

Coefficients	68% confidence interval		95% confidence interval	
(TeV^{-2})	Expected	Observed	Expected	Observed
c_{WWW}/Λ^2	$[-1.8, 1.8]$	$[-0.93, 0.99]$	$[-2.7, 2.7]$	$[-1.8, 1.8]$
c_W/Λ^2	$[-3.7, 2.7]$	$[-2.0, 1.3]$	$[-5.3, 4.2]$	$[-3.6, 2.8]$
c_B/Λ^2	$[-9.4, 8.4]$	$[-5.1, 4.3]$	$[-14, 13]$	$[-9.4, 8.5]$

considered here; the 0- and 1-jet categories have been combined. The corresponding 68% and 95% C.L. intervals are reported in Table IX. The observed limits are stronger than expected due to a deficit of events at high $m_{e\mu}$. In all cases, they are within 2 standard deviations of the expected limits as determined by pseudoexperiments. The observed limits are about a factor of 2 more stringent than recent results reported by the ATLAS Collaboration [7] and the previous W^+W^- results from the CMS Collaboration [5]. The sensitivity of this analysis to c_{WWW} and c_W is similar to the CMS WZ analysis [59] and is much better for c_B. Finally, the sensitivity is slightly weaker than for the CMS analysis of W^+W^- and WZ production in lepton and jets events [60]. Figure 10 (right) shows the expected and observed 68% and 95% confidence level contours for pairs of Wilson coefficients.

XIII. SUMMARY

Measurements of W^+W^- boson pair production in proton-proton collisions at $\sqrt{s} = 13$ TeV were performed. The analysis is based on data collected with the CMS detector at the LHC corresponding to an integrated luminosity of 35.9 fb^{-1}. Candidate events were selected that have two leptons (electrons or muons) with opposite charges. Two analysis methods were described. The first method imposes a sequence of requirements on kinematic quantities to suppress backgrounds, while the second uses a pair of random forest classifiers. The total production cross section is $\sigma_{SC}^{tot} = 117.6 \pm 1.4(\text{stat}) \pm 5.5(\text{syst}) \pm 1.9(\text{theo}) \pm 3.2(\text{lumi})$ pb $= 117.6 \pm 6.8$ pb, where the individual uncertainties are statistical, experimental systematic, theoretical, and of integrated luminosity; this measured value is consistent with the next-to-next-to-leading-order theoretical prediction 118.8 ± 3.6 pb. Fiducial cross sections are also measured including the change in the 0-jet fiducial cross section with jet transverse momentum threshold. Normalized differential cross sections are measured and compared with next-to-leading-order SM predictions. Good agreement is observed. The normalized jet multiplicity distribution in W^+W^- events is measured. Finally, bounds on coefficients of dimension-6 operators in the context of an effective field theory are set using electron-muon invariant mass distributions.

[1] V. M. Abazov *et al.* (D0 Collaboration), Measurement of the *WW* Production Cross Section with Dilepton Final States in p$\bar{\text{p}}$ Collisions at $\sqrt{s} = 1.96$ TeV and Limits on Anomalous Trilinear Gauge Couplings, Phys. Rev. Lett. **103,** 191801 (2009).

[2] T. Aaltonen *et al.* (CDF Collaboration), Measurement of the W^+W^- Production Cross Section and Search for Anomalous WWγ and WWZ Couplings in p$\bar{\text{p}}$ Collisions at $\sqrt{s} = 1.96$ TeV, Phys. Rev. Lett. **104,** 201801 (2010).

[3] ATLAS Collaboration, Measurement of W^+W^- production in pp collisions at $\sqrt{s} = 7$ TeV with the ATLAS detector and limits on anomalous WWZ and WWγ couplings, Phys. Rev. D **87,** 112001 (2013); Erratum, Phys. Rev. D **88,** 079906 (2013).

[4] CMS Collaboration, Measurement of the W^+W^- cross section in pp collisions at $\sqrt{s} = 7$ TeV and limits on anomalous WWγ and WWZ couplings, Eur. Phys. J. C **73,** 2610 (2013).

[5] CMS Collaboration, Measurement of the W^+W^- cross section in pp collisions at $\sqrt{s} = 8$ TeV and limits on anomalous gauge couplings, Eur. Phys. J. C **76,** 401 (2016).

[6] ATLAS Collaboration, Measurement of total and differential W^+W^- production cross sections in proton-proton collisions at $\sqrt{s} = 8$ TeV with the ATLAS detector and limits on anomalous triple-gauge-boson couplings, J. High Energy Phys. 09 (2016) 029.

[7] ATLAS Collaboration, Measurement of fiducial and differential W^+W^- production cross sections at $\sqrt{s} = 13$ TeV with the ATLAS detector, Eur. Phys. J. C **79,** 884 (2019).

[8] T. Gehrmann, M. Grazzini, S. Kallweit, P. Maierhöfer, A. von Manteuffel, S. Pozzorini, D. Rathlev, and L. Tancredi, W^+W^- Production at Hadron Colliders in Next-to-Next-to-Leading-Order QCD, Phys. Rev. Lett. **113,** 212001 (2014).

[9] F. Caola, K. Melnikov, R. Röntsch, and L. Tancredi, QCD corrections to W^+W^- production through gluon fusion, Phys. Lett. B **754,** 275 (2016).

[10] S. Gieseke, T. Kasprzik, and J. H. Kühn, Vector-boson pair production and electroweak corrections in HERWIG++, Eur. Phys. J. C **74,** 2988 (2014).

[11] L. Breiman, Random Forests, Mach. Learn. **45,** 5 (2001).

[12] T. K. Ho, The random subspace method for constructing decision forests, IEEE Trans. Pattern Anal. Mach. Intell. **20,** 832 (1998).

[13] R. Caruana and A. Niculescu-Mizil, An empirical comparison of supervised learning algorithms using different performance metrics, in *Proceedings of the 23rd International Conference on Machine Learning (ICML'06)* (IEEE, 2005), p. 161.

[14] S. Weinberg, Phenomenological Lagrangians, Physica (Amsterdam) **96A,** 327 (1979).

[15] C. Degrande, N. Greiner, W. Kilian, O. Mattelaer, H. Mebane, T. Stelzer, S. Willenbrock, and C. Zhang, Effective field theory: A modern approach to anomalous couplings, Ann. Phys. (Amsterdam) **335,** 21 (2013).

[16] CMS Collaboration, The CMS trigger system, J. Instrum. **12,** P01020 (2017).

[17] CMS Collaboration, The CMS Experiment at the CERN LHC, J. Instrum. **3,** S08004 (2008).

[18] P. Nason, A new method for combining NLO QCD with shower Monte Carlo algorithms, J. High Energy Phys. 11 (2004) 040.

[19] S. Frixione, P. Nason, and C. Oleari, Matching NLO QCD computations with parton shower simulations: The POWHEG method, J. High Energy Phys. 11 (2007) 070.

[20] S. Alioli, P. Nason, C. Oleari, and E. Re, A general framework for implementing NLO calculations in shower Monte Carlo programs: The POWHEG BOX, J. High Energy Phys. 06 (2010) 043.

[21] P. Nason and G. Zanderighi, W^+W^-, WZ and ZZ production in the POWHEG-BOX-V2, Eur. Phys. J. C **74,** 2702 (2014).

[22] S. Alioli, P. Nason, C. Oleari, and E. Re, NLO vector-boson production matched with shower in POWHEG, J. High Energy Phys. 07 (2008) 060.

[23] S. Alioli, P. Nason, C. Oleari, and E. Re, NLO Higgs boson production via gluon fusion matched with shower in POWHEG, J. High Energy Phys. 04 (2009) 002.

[24] J. M. Campbell and R. K. Ellis, MCFM for the tevatron and the LHC, Nucl. Phys. B, Proc. Suppl. **205–206,** 10 (2010).

[25] Y. Gao, A. V. Gritsan, Z. Guo, K. Melnikov, M. Schulze, and N. V. Tran, Spin determination of single-produced resonances at hadron colliders, Phys. Rev. D **81**, 075022 (2010); Erratum, Phys. Rev. D **81**, 079905 (2010).

[26] J. Alwall, R. Frederix, S. Frixione, V. Hirschi, F. Maltoni, O. Mattelaer, H. S. Shao, T. Stelzer, P. Torrielli, and M. Zaro, The automated computation of tree-level and next-to-leading order differential cross sections, and their matching to parton shower simulations, J. High Energy Phys. 07 (2014) 079.

[27] J. M. Campbell, R. K. Ellis, P. Nason, and E. Re, Top-pair production and decay at NLO matched with parton showers, J. High Energy Phys. 04 (2015) 114.

[28] E. Re, Single-top *Wt*-channel production matched with parton showers using the POWHEG method, Eur. Phys. J. C **71**, 1547 (2011).

[29] T. Sjöstrand, S. Mrenna, and P. Z. Skands, An introduction to PYTHIA 8.2, Comput. Phys. Commun. **191**, 159 (2015).

[30] CMS Collaboration, Event generator tunes obtained from underlying event and multiparton scattering measurements, Eur. Phys. J. C **76**, 155 (2016).

[31] R. D. Ball, V. Bertone, S. Carrazza, C. Deans, L. Del Debbio, S. Forte, A. Guffanti, N. Hartland, J. Latorre, J. Rojo, and M. Ubiali (NNPDF Collaboration), Parton distributions with LHC data, Nucl. Phys. **B867**, 244 (2013).

[32] R. D. Ball *et al.* (NNPDF Collaboration), Parton distributions for the LHC Run II, J. High Energy Phys. 04 (2015) 040.

[33] CMS Collaboration, Investigations of the impact of the parton shower tuning in PYTHIA8 in the modelling of $t\bar{t}$ at $\sqrt{s} = 8$ and 13 TeV, CMS physics analysis summary CMS-PAS-TOP-16-021, 2016.

[34] S. Agostinelli *et al.* (GEANT4 Collaboration), GEANT4—A simulation toolkit, Nucl. Instrum. Methods Phys. Res., Sect. A **506**, 250 (2003).

[35] CMS Collaboration, Particle-flow reconstruction and global event description with the CMS detector, J. Instrum. **12**, P10003 (2017).

[36] M. Cacciari, G. P. Salam, and G. Soyez, The anti-k_T jet clustering algorithm, J. High Energy Phys. 04 (2008) 063.

[37] M. Cacciari, G. P. Salam, and G. Soyez, FastJet user manual, Eur. Phys. J. C **72**, 1896 (2012).

[38] CMS Collaboration, Jet performance in *pp* collisions at 7 TeV, CMS physics analysis summary CMS-PAS-JME-10-003, 2010.

[39] CMS Collaboration, Pileup mitigation at CMS in 13 TeV data, J. Instrum. **15**, P09018 (2020).

[40] CMS Collaboration, Identification of *b*-quark jets with the CMS experiment, J. Instrum. **8**, P04013 (2013).

[41] CMS Collaboration, Identification of heavy-flavour jets with the CMS detector in *pp* collisions at 13 TeV, J. Instrum. **13**, P05011 (2018).

[42] CMS Collaboration, Performance of electron reconstruction and selection with the CMS detector in proton-proton collisions at $\sqrt{s} = 8$ TeV, J. Instrum. **10**, P06005 (2015).

[43] CMS Collaboration, The performance of the CMS muon detector in proton-proton collisions at $\sqrt{s} = 7$ TeV at the LHC, J. Instrum. **8**, P11002 (2013).

[44] CMS Collaboration, Performance of the CMS muon detector and muon reconstruction with proton-proton collisions at $\sqrt{s} = 13$ TeV, J. Instrum. **13**, P06015 (2018).

[45] H. Voss, A. Höcker, J. Stelzer, and F. Tegenfeldt, in *XIth International Workshop on Advanced Computing and Analysis Techniques in Physics Research (ACAT)* (2007), p. 40; TMVA, the toolkit for multivariate data analysis with ROOT, Proc. Sci. (ACAT) 040.

[46] CMS Collaboration, Measurement of Higgs boson production and properties in the *WW* decay channel with leptonic final states, J. High Energy Phys. 01 (2014) 096.

[47] CMS Collaboration, Measurements of properties of the Higgs boson decaying to a *W* boson pair in *pp* collisions at $\sqrt{s} = 13$ TeV, Phys. Lett. B **791**, 96 (2019).

[48] CMS Collaboration, Jet energy scale and resolution in the CMS experiment in *pp* collisions at 8 TeV, J. Instrum. **12**, P02014 (2017).

[49] CMS Collaboration, Measurement of the inelastic proton-proton cross section at $\sqrt{s} = 13$ TeV, J. High Energy Phys. 07 (2018) 161.

[50] CMS Collaboration, CMS luminosity measurements for the 2016 data taking period, CMS physics analysis summary CMS-PAS-LUM-17-001 (2016).

[51] M. Grazzini, S. Kallweit, D. Rathlev, and M. Wiesemann, Transverse-momentum resummation for vector-boson pair production at NNLL + NNLO, J. High Energy Phys. 08 (2015) 154.

[52] P. Meade, H. Ramani, and M. Zeng, Transverse momentum resummation effects in W^+W^- measurements, Phys. Rev. D **90**, 114006 (2014).

[53] P. Jaiswal and T. Okui, Explanation of the *WW* excess at the LHC by jet-veto resummation, Phys. Rev. D **90**, 073009 (2014).

[54] P. Jaiswal, P. Meade, and H. Ramani, Precision diboson measurements and the interplay of p_T and jet-veto resummations, Phys. Rev. D **93**, 093007 (2016).

[55] J. Butterworth *et al.*, PDF4LHC recommendations for LHC Run II, J. Phys. G **43**, 023001 (2016).

[56] M. Tanabashi (Particle Data Group) *et al.*, Review of particle physics, Phys. Rev. D **98**, 030001 (2018).

[57] W. Buchmüller and D. Wyler, Effective Lagrangian analysis of new interactions and flavor conservation, Nucl. Phys. **B268**, 621 (1986).

[58] B. Grzadkowski, M. Iskrzyński, M. Misiak, and J. Rosiek, Dimension-six terms in the standard model Lagrangian, J. High Energy Phys. 10 (2010) 085.

[59] CMS Collaboration, Measurements of the $pp \rightarrow WZ$ inclusive and differential production cross section and constraints on charged anomalous triple gauge couplings at $\sqrt{s} = 13$ TeV, J. High Energy Phys. 04 (2019) 122.

[60] CMS Collaboration, Search for anomalous triple gauge couplings in *WW* and *WZ* production in lepton + jet events in proton-proton collisions at $\sqrt{s} = 13$ TeV, J. High Energy Phys. 12 (2019) 062.

A. M. Sirunyan,[1,a] A. Tumasyan,[1] W. Adam,[2] F. Ambrogi,[2] T. Bergauer,[2] M. Dragicevic,[2] J. Erö,[2] A. Escalante Del Valle,[2] R. Frühwirth,[2,b] M. Jeitler,[2,b] N. Krammer,[2] L. Lechner,[2] D. Liko,[2] T. Madlener,[2] I. Mikulec,[2] F. M. Pitters,[2] N. Rad,[2] J. Schieck,[2,b] R. Schöfbeck,[2] M. Spanring,[2] S. Templ,[2] W. Waltenberger,[2] C.-E. Wulz,[2,b] M. Zarucki,[2] V. Chekhovsky,[3] A. Litomin,[3] V. Makarenko,[3] J. Suarez Gonzalez,[3] M. R. Darwish,[4,c] E. A. De Wolf,[4] D. Di Croce,[4] X. Janssen,[4] T. Kello,[4,d] A. Lelek,[4] M. Pieters,[4] H. Rejeb Sfar,[4] H. Van Haevermaet,[4] P. Van Mechelen,[4] S. Van Putte,[4] N. Van Remortel,[4] F. Blekman,[5] E. S. Bols,[5] S. S. Chhibra,[5] J. D'Hondt,[5] J. De Clercq,[5] D. Lontkovskyi,[5] S. Lowette,[5] I. Marchesini,[5] S. Moortgat,[5] A. Morton,[5] Q. Python,[5] S. Tavernier,[5] W. Van Doninck,[5] P. Van Mulders,[5] D. Beghin,[6] B. Bilin,[6] B. Clerbaux,[6] G. De Lentdecker,[6] H. Delannoy,[6] B. Dorney,[6] L. Favart,[6] A. Grebenyuk,[6] A. K. Kalsi,[6] I. Makarenko,[6] L. Moureaux,[6] L. Pétré,[6] A. Popov,[6] N. Postiau,[6] E. Starling,[6] L. Thomas,[6] C. Vander Velde,[6] P. Vanlaer,[6] D. Vannerom,[6] L. Wezenbeek,[6] T. Cornelis,[7] D. Dobur,[7] M. Gruchala,[7] I. Khvastunov,[7,e] M. Niedziela,[7] C. Roskas,[7] K. Skovpen,[7] M. Tytgat,[7] W. Verbeke,[7] B. Vermassen,[7] M. Vit,[7] G. Bruno,[8] F. Bury,[8] C. Caputo,[8] P. David,[8] C. Delaere,[8] M. Delcourt,[8] I. S. Donertas,[8] A. Giammanco,[8] V. Lemaitre,[8] K. Mondal,[8] J. Prisciandaro,[8] A. Taliercio,[8] M. Teklishyn,[8] P. Vischia,[8] S. Wuyckens,[8] J. Zobec,[8] G. A. Alves,[9] G. Correia Silva,[9] C. Hensel,[9] A. Moraes,[9] W. L. Aldá Júnior,[10] E. Belchior Batista Das Chagas,[10] H. Brandao Malbouisson,[10] W. Carvalho,[10] J. Chinellato,[10,f] E. Coelho,[10] E. M. Da Costa,[10] G. G. Da Silveira,[10,g] D. De Jesus Damiao,[10] S. Fonseca De Souza,[10] J. Martins,[10,h] D. Matos Figueiredo,[10] M. Medina Jaime,[10,i] M. Melo De Almeida,[10] C. Mora Herrera,[10] L. Mundim,[10] H. Nogima,[10] P. Rebello Teles,[10] L. J. Sanchez Rosas,[10] A. Santoro,[10] S. M. Silva Do Amaral,[10] A. Sznajder,[10] M. Thiel,[10] E. J. Tonelli Manganote,[10,f] F. Torres Da Silva De Araujo,[10] A. Vilela Pereira,[10] C. A. Bernardes,[11a] L. Calligaris,[11a] T. R. Fernandez Perez Tomei,[11a] E. M. Gregores,[11a,11b] D. S. Lemos,[11a] P. G. Mercadante,[11a,11b] S. F. Novaes,[11a] Sandra S. Padula,[11a] A. Aleksandrov,[12] G. Antchev,[12] I. Atanasov,[12] R. Hadjiiska,[12] P. Iaydjiev,[12] M. Misheva,[12] M. Rodozov,[12] M. Shopova,[12] G. Sultanov,[12] M. Bonchev,[13] A. Dimitrov,[13] T. Ivanov,[13] L. Litov,[13] B. Pavlov,[13] P. Petkov,[13] A. Petrov,[13] W. Fang,[14,d] Q. Guo,[14] H. Wang,[14] L. Yuan,[14] M. Ahmad,[15] Z. Hu,[15] Y. Wang,[15] E. Chapon,[16] G. M. Chen,[16,j] H. S. Chen,[16,j] M. Chen,[16] D. Leggat,[16] H. Liao,[16] Z. Liu,[16] R. Sharma,[16] A. Spiezia,[16] J. Tao,[16] J. Thomas-wilsker,[16] J. Wang,[16] H. Zhang,[16] S. Zhang,[16,j] J. Zhao,[16] A. Agapitos,[17] Y. Ban,[17] C. Chen,[17] A. Levin,[17] J. Li,[17] Q. Li,[17] M. Lu,[17] X. Lyu,[17] Y. Mao,[17] S. J. Qian,[17] D. Wang,[17] Q. Wang,[17] J. Xiao,[17] Z. You,[18] X. Gao,[19,d] M. Xiao,[20] C. Avila,[21] A. Cabrera,[21] C. Florez,[21] J. Fraga,[21] A. Sarkar,[21] M. A. Segura Delgado,[21] J. Jaramillo,[22] J. Mejia Guisao,[22] F. Ramirez,[22] J. D. Ruiz Alvarez,[22] C. A. Salazar González,[22] N. Vanegas Arbelaez,[22] D. Giljanovic,[23] N. Godinovic,[23] D. Lelas,[23] I. Puljak,[23] T. Sculac,[23] Z. Antunovic,[24] M. Kovac,[24] V. Brigljevic,[25] D. Ferencek,[25] D. Majumder,[25] B. Mesic,[25] M. Roguljic,[25] A. Starodumov,[25,k] T. Susa,[25] M. W. Ather,[26] A. Attikis,[26] E. Erodotou,[26] A. Ioannou,[26] G. Kole,[26] M. Kolosova,[26] S. Konstantinou,[26] G. Mavromanolakis,[26] J. Mousa,[26] C. Nicolaou,[26] F. Ptochos,[26] P. A. Razis,[26] H. Rykaczewski,[26] H. Saka,[26] D. Tsiakkouri,[26] M. Finger,[27,l] M. Finger Jr.,[27,l] A. Kveton,[27] J. Tomsa,[27] E. Ayala,[28] E. Carrera Jarrin,[29] A. A. Abdelalim,[30,m,n] S. Abu Zeid,[30,o] S. Khalil,[30,m] A. Lotfy,[31] M. A. Mahmoud,[31] S. Bhowmik,[32] A. Carvalho Antunes De Oliveira,[32] R. K. Dewanjee,[32] K. Ehataht,[32] M. Kadastik,[32] M. Raidal,[32] C. Veelken,[32] P. Eerola,[33] L. Forthomme,[33] H. Kirschenmann,[33] K. Osterberg,[33] M. Voutilainen,[33] E. Brücken,[34] F. Garcia,[34] J. Havukainen,[34] V. Karimäki,[34] M. S. Kim,[34] R. Kinnunen,[34] T. Lampén,[34] K. Lassila-Perini,[34] S. Laurila,[34] S. Lehti,[34] T. Lindén,[34] H. Siikonen,[34] E. Tuominen,[34] J. Tuominiemi,[34] P. Luukka,[35] T. Tuuva,[35] M. Besancon,[36] F. Couderc,[36] M. Dejardin,[36] D. Denegri,[36] J. L. Faure,[36] F. Ferri,[36] S. Ganjour,[36] A. Givernaud,[36] P. Gras,[36] G. Hamel de Monchenault,[36] P. Jarry,[36] B. Lenzi,[36] E. Locci,[36] J. Malcles,[36] J. Rander,[36] A. Rosowsky,[36] M. Ö. Sahin,[36] A. Savoy-Navarro,[36,p] M. Titov,[36] G. B. Yu,[36] S. Ahuja,[37] C. Amendola,[37] F. Beaudette,[37] M. Bonanomi,[37] P. Busson,[37] C. Charlot,[37] O. Davignon,[37] B. Diab,[37] G. Falmagne,[37] R. Granier de Cassagnac,[37] I. Kucher,[37] A. Lobanov,[37] C. Martin Perez,[37] M. Nguyen,[37] C. Ochando,[37] P. Paganini,[37] J. Rembser,[37] R. Salerno,[37] J. B. Sauvan,[37] Y. Sirois,[37] A. Zabi,[37] A. Zghiche,[37] J.-L. Agram,[38,q] J. Andrea,[38] D. Bloch,[38] G. Bourgatte,[38] J.-M. Brom,[38] E. C. Chabert,[38] C. Collard,[38] J.-C. Fontaine,[38,q] D. Gelé,[38] U. Goerlach,[38] C. Grimault,[38] A.-C. Le Bihan,[38] P. Van Hove,[38] E. Asilar,[39] S. Beauceron,[39] C. Bernet,[39] G. Boudoul,[39] C. Camen,[39] A. Carle,[39] N. Chanon,[39] D. Contardo,[39] P. Depasse,[39] H. El Mamouni,[39] J. Fay,[39] S. Gascon,[39] M. Gouzevitch,[39] B. Ille,[39] Sa. Jain,[39] I. B. Laktineh,[39] H. Lattaud,[39] A. Lesauvage,[39] M. Lethuillier,[39] L. Mirabito,[39] L. Torterotot,[39] G. Touquet,[39] M. Vander Donckt,[39] S. Viret,[39] T. Toriashvili,[40,r] Z. Tsamalaidze,[40,l] L. Feld,[41] K. Klein,[41] M. Lipinski,[41] D. Meuser,[41] A. Pauls,[41] M. Preuten,[41] M. P. Rauch,[41] J. Schulz,[41] M. Teroerde,[41] D. Eliseev,[42] M. Erdmann,[42] P. Fackeldey,[42] B. Fischer,[42] S. Ghosh,[42] T. Hebbeker,[42] K. Hoepfner,[42] H. Keller,[42] L. Mastrolorenzo,[42] M. Merschmeyer,[42] A. Meyer,[42] P. Millet,[42] G. Mocellin,[42] S. Mondal,[42] S. Mukherjee,[42] D. Noll,[42] A. Novak,[42] T. Pook,[42] A. Pozdnyakov,[42] T. Quast,[42]

M. Radziej,[42] Y. Rath,[42] H. Reithler,[42] J. Roemer,[42] A. Schmidt,[42] S. C. Schuler,[42] A. Sharma,[42] S. Wiedenbeck,[42]
S. Zaleski,[42] C. Dziwok,[43] G. Flügge,[43] W. Haj Ahmad,[43,s] O. Hlushchenko,[43] T. Kress,[43] A. Nowack,[43] C. Pistone,[43]
O. Pooth,[43] D. Roy,[43] H. Sert,[43] A. Stahl,[43,t] T. Ziemons,[43] H. Aarup Petersen,[44] M. Aldaya Martin,[44] P. Asmuss,[44]
I. Babounikau,[44] S. Baxter,[44] O. Behnke,[44] A. Bermúdez Martínez,[44] A. A. Bin Anuar,[44] K. Borras,[44,u] V. Botta,[44]
D. Brunner,[44] A. Campbell,[44] A. Cardini,[44] P. Connor,[44] S. Consuegra Rodríguez,[44] V. Danilov,[44] A. De Wit,[44]
M. M. Defranchis,[44] L. Didukh,[44] D. Domínguez Damiani,[44] G. Eckerlin,[44] D. Eckstein,[44] T. Eichhorn,[44] A. Elwood,[44]
L. I. Estevez Banos,[44] E. Gallo,[44,v] A. Geiser,[44] A. Giraldi,[44] A. Grohsjean,[44] M. Guthoff,[44] A. Harb,[44] A. Jafari,[44,w]
N. Z. Jomhari,[44] H. Jung,[44] A. Kasem,[44,u] M. Kasemann,[44] H. Kaveh,[44] J. Keaveney,[44] C. Kleinwort,[44] J. Knolle,[44]
D. Krücker,[44] W. Lange,[44] T. Lenz,[44] J. Lidrych,[44] K. Lipka,[44] W. Lohmann,[44,x] R. Mankel,[44] I.-A. Melzer-Pellmann,[44]
J. Metwally,[44] A. B. Meyer,[44] M. Meyer,[44] M. Missiroli,[44] J. Mnich,[44] A. Mussgiller,[44] V. Myronenko,[44] Y. Otarid,[44]
D. Pérez Adán,[44] S. K. Pflitsch,[44] D. Pitzl,[44] A. Raspereza,[44] A. Saggio,[44] A. Saibel,[44] M. Savitskyi,[44] V. Scheurer,[44]
P. Schütze,[44] C. Schwanenberger,[44] R. Shevchenko,[44] A. Singh,[44] R. E. Sosa Ricardo,[44] H. Tholen,[44] N. Tonon,[44]
O. Turkot,[44] A. Vagnerini,[44] M. Van De Klundert,[44] R. Walsh,[44] D. Walter,[44] Y. Wen,[44] K. Wichmann,[44] C. Wissing,[44]
S. Wuchterl,[44] O. Zenaiev,[44] R. Zlebcik,[44] R. Aggleton,[45] S. Bein,[45] L. Benato,[45] A. Benecke,[45] K. De Leo,[45] T. Dreyer,[45]
A. Ebrahimi,[45] F. Feindt,[45] A. Fröhlich,[45] C. Garbers,[45] E. Garutti,[45] D. Gonzalez,[45] P. Gunnellini,[45] J. Haller,[45]
A. Hinzmann,[45] A. Karavdina,[45] G. Kasieczka,[45] R. Klanner,[45] R. Kogler,[45] S. Kurz,[45] V. Kutzner,[45] J. Lange,[45] T. Lange,[45]
A. Malara,[45] J. Multhaup,[45] C. E. N. Niemeyer,[45] A. Nigamova,[45] K. J. Pena Rodriguez,[45] O. Rieger,[45] P. Schleper,[45]
S. Schumann,[45] J. Schwandt,[45] D. Schwarz,[45] J. Sonneveld,[45] H. Stadie,[45] G. Steinbrück,[45] B. Vormwald,[45] I. Zoi,[45]
M. Baselga,[46] S. Baur,[46] J. Bechtel,[46] T. Berger,[46] E. Butz,[46] R. Caspart,[46] T. Chwalek,[46] W. De Boer,[46] A. Dierlamm,[46]
A. Droll,[46] K. El Morabit,[46] N. Faltermann,[46] K. Flöh,[46] M. Giffels,[46] A. Gottmann,[46] F. Hartmann,[46,t] C. Heidecker,[46]
U. Husemann,[46] M. A. Iqbal,[46] I. Katkov,[46,y] P. Keicher,[46] R. Koppenhöfer,[46] S. Kudella,[46] S. Maier,[46] M. Metzler,[46]
S. Mitra,[46] M. U. Mozer,[46] D. Müller,[46] Th. Müller,[46] M. Musich,[46] G. Quast,[46] K. Rabbertz,[46] J. Rauser,[46] D. Savoiu,[46]
D. Schäfer,[46] M. Schnepf,[46] M. Schröder,[46] D. Seith,[46] I. Shvetsov,[46] H. J. Simonis,[46] R. Ulrich,[46] M. Wassmer,[46]
M. Weber,[46] C. Wöhrmann,[46] R. Wolf,[46] S. Wozniewski,[46] G. Anagnostou,[47] P. Asenov,[47] G. Daskalakis,[47] T. Geralis,[47]
A. Kyriakis,[47] D. Loukas,[47] G. Paspalaki,[47] A. Stakia,[47] M. Diamantopoulou,[48] D. Karasavvas,[48] G. Karathanasis,[48]
P. Kontaxakis,[48] C. K. Koraka,[48] A. Manousakis-katsikakis,[48] A. Panagiotou,[48] I. Papavergou,[48] N. Saoulidou,[48]
K. Theofilatos,[48] K. Vellidis,[48] E. Vourliotis,[48] G. Bakas,[49] K. Kousouris,[49] I. Papakrivopoulos,[49] G. Tsipolitis,[49]
A. Zacharopoulou,[49] I. Evangelou,[50] C. Foudas,[50] P. Gianneios,[50] P. Katsoulis,[50] P. Kokkas,[50] S. Mallios,[50] K. Manitara,[50]
N. Manthos,[50] I. Papadopoulos,[50] J. Strologas,[50] M. Bartók,[51,z] R. Chudasama,[51] M. Csanad,[51] M. M. A. Gadallah,[51,aa]
S. Lökös,[51,bb] P. Major,[51] K. Mandal,[51] A. Mehta,[51] G. Pasztor,[51] O. Surányi,[51] G. I. Veres,[51] G. Bencze,[52] C. Hajdu,[52]
D. Horvath,[52,cc] F. Sikler,[52] V. Veszpremi,[52] G. Vesztergombi,[52,a,bb] S. Czellar,[53] J. Karancsi,[53,z] J. Molnar,[53] Z. Szillasi,[53]
D. Teyssier,[53] P. Raics,[54] Z. L. Trocsanyi,[54] B. Ujvari,[54] T. Csorgo,[55] F. Nemes,[55] T. Novak,[55] S. Choudhury,[56]
J. R. Komaragiri,[56] D. Kumar,[56] L. Panwar,[56] P. C. Tiwari,[56] S. Bahinipati,[57,dd] D. Dash,[57] C. Kar,[57] P. Mal,[57] T. Mishra,[57]
V. K. Muraleedharan Nair Bindhu,[57] A. Nayak,[57,ee] D. K. Sahoo,[57,dd] N. Sur,[57] S. K. Swain,[57] S. Bansal,[58] S. B. Beri,[58]
V. Bhatnagar,[58] S. Chauhan,[58] N. Dhingra,[58,ff] R. Gupta,[58] A. Kaur,[58] A. Kaur,[58] S. Kaur,[58] P. Kumari,[58] M. Lohan,[58]
M. Meena,[58] K. Sandeep,[58] S. Sharma,[58] J. B. Singh,[58] A. K. Virdi,[58] A. Ahmed,[59] A. Bhardwaj,[59] B. C. Choudhary,[59]
R. B. Garg,[59] M. Gola,[59] S. Keshri,[59] A. Kumar,[59] M. Naimuddin,[59] P. Priyanka,[59] K. Ranjan,[59] A. Shah,[59] M. Bharti,[60,gg]
R. Bhattacharya,[60] S. Bhattacharya,[60] D. Bhowmik,[60] S. Dutta,[60] S. Ghosh,[60] B. Gomber,[60,hh] M. Maity,[60,ii] S. Nandan,[60]
P. Palit,[60] A. Purohit,[60] P. K. Rout,[60] G. Saha,[60] S. Sarkar,[60] M. Sharan,[60] B. Singh,[60,gg] S. Thakur,[60,gg] P. K. Behera,[61]
S. C. Behera,[61] P. Kalbhor,[61] A. Muhammad,[61] R. Pradhan,[61] P. R. Pujahari,[61] A. Sharma,[61] A. K. Sikdar,[61] D. Dutta,[62]
V. Jha,[62] V. Kumar,[62] D. K. Mishra,[62] K. Naskar,[62,jj] P. K. Netrakanti,[62] L. M. Pant,[62] P. Shukla,[62] T. Aziz,[63] M. A. Bhat,[63]
S. Dugad,[63] R. Kumar Verma,[63] U. Sarkar,[63] S. Banerjee,[64] S. Bhattacharya,[64] S. Chatterjee,[64] P. Das,[64] M. Guchait,[64]
S. Karmakar,[64] S. Kumar,[64] G. Majumder,[64] K. Mazumdar,[64] S. Mukherjee,[64] D. Roy,[64] N. Sahoo,[64] S. Dube,[65] B. Kansal,[65]
A. Kapoor,[65] K. Kothekar,[65] S. Pandey,[65] A. Rane,[65] A. Rastogi,[65] S. Sharma,[65] H. Bakhshiansohi,[66,kk] S. Chenarani,[67,ll]
S. M. Etesami,[67] M. Khakzad,[67] M. Mohammadi Najafabadi,[67] M. Naseri,[67] M. Felcini,[68] M. Grunewald,[68]
M. Abbrescia,[69a,69b] R. Aly,[69a,69b,mm] C. Aruta,[69a,69b] A. Colaleo,[69a] D. Creanza,[69a,69c] N. De Filippis,[69a,69c]
M. De Palma,[69a,69b] A. Di Florio,[69a,69b] A. Di Pilato,[69a,69b] W. Elmetenawee,[69a,69b] L. Fiore,[69a] A. Gelmi,[69a,69b] M. Gul,[69a]
G. Iaselli,[69a,69c] M. Ince,[69a,69b] S. Lezki,[69a,69b] G. Maggi,[69a,69c] M. Maggi,[69a] I. Margjeka,[69a,69b] J. A. Merlin,[69a] S. My,[69a,69b]
S. Nuzzo,[69a,69b] A. Pompili,[69a,69b] G. Pugliese,[69a,69c] A. Ranieri,[69a] G. Selvaggi,[69a,69b] L. Silvestris,[69a] F. M. Simone,[69a,69b]

R. Venditti,[69a] P. Verwilligen,[69a] G. Abbiendi,[70a] C. Battilana,[70a,70b] D. Bonacorsi,[70a,70b] L. Borgonovi,[70a,70b] S. Braibant-Giacomelli,[70a,70b] R. Campanini,[70a,70b] P. Capiluppi,[70a,70b] A. Castro,[70a,70b] F. R. Cavallo,[70a] M. Cuffiani,[70a,70b] G. M. Dallavalle,[70a] T. Diotalevi,[70a,70b] F. Fabbri,[70a] A. Fanfani,[70a,70b] E. Fontanesi,[70a,70b] P. Giacomelli,[70a] L. Giommi,[70a,70b] C. Grandi,[70a] L. Guiducci,[70a,70b] F. Iemmi,[70a,70b] S. Lo Meo,[70a,nn] S. Marcellini,[70a] G. Masetti,[70a] F. L. Navarria,[70a,70b] A. Perrotta,[70a] F. Primavera,[70a,70b] A. M. Rossi,[70a,70b] T. Rovelli,[70a,70b] G. P. Siroli,[70a,70b] N. Tosi,[70a] S. Albergo,[71a,71b,oo] S. Costa,[71a,71b] A. Di Mattia,[71a] R. Potenza,[71a,71b] A. Tricomi,[71a,71b,oo] C. Tuve,[71a,71b] G. Barbagli,[72a] A. Cassese,[72a] R. Ceccarelli,[72a,72b] V. Ciulli,[72a,72b] C. Civinini,[72a] R. D'Alessandro,[72a,72b] F. Fiori,[72a] E. Focardi,[72a,72b] G. Latino,[72a,72b] P. Lenzi,[72a,72b] M. Lizzo,[72a,72b] M. Meschini,[72a] S. Paoletti,[72a] R. Seidita,[72a,72b] G. Sguazzoni,[72a] L. Viliani,[72a] L. Benussi,[73] S. Bianco,[73] D. Piccolo,[73] M. Bozzo,[74a,74b] F. Ferro,[74a] R. Mulargia,[74a,74b] E. Robutti,[74a] S. Tosi,[74a,74b] A. Benaglia,[75a] A. Beschi,[75a,75b] F. Brivio,[75a,75b] F. Cetorelli,[75a,75b] V. Ciriolo,[75a,75b,t] F. De Guio,[75a,75b] M. E. Dinardo,[75a,75b] P. Dini,[75a] S. Gennai,[75a] A. Ghezzi,[75a,75b] P. Govoni,[75a,75b] L. Guzzi,[75a,75b] M. Malberti,[75a] S. Malvezzi,[75a] D. Menasce,[75a] F. Monti,[75a,75b] L. Moroni,[75a] M. Paganoni,[75a,75b] D. Pedrini,[75a] S. Ragazzi,[75a,75b] T. Tabarelli de Fatis,[75a,75b] D. Valsecchi,[75a,75b,t] D. Zuolo,[75a,75b] S. Buontempo,[76a] N. Cavallo,[76a,76c] A. De Iorio,[76a,76b] F. Fabozzi,[76a,76c] F. Fienga,[76a] A. O. M. Iorio,[76a,76b] L. Layer,[76a,76b] L. Lista,[76a,76b] S. Meola,[76a,76d,t] P. Paolucci,[76a,t] B. Rossi,[76a] C. Sciacca,[76a,76b] E. Voevodina,[76a,76b] P. Azzi,[77a] N. Bacchetta,[77a] D. Bisello,[77a,77b] A. Boletti,[77a,77b] A. Bragagnolo,[77a,77b] R. Carlin,[77a,77b] P. Checchia,[77a] P. De Castro Manzano,[77a] T. Dorigo,[77a] F. Gasparini,[77a,77b] S. Y. Hoh,[77a,77b] M. Margoni,[77a,77b] A. T. Meneguzzo,[77a,77b] M. Presilla,[77a,77b] P. Ronchese,[77a,77b] R. Rossin,[77a,77b] F. Simonetto,[77a,77b] G. Strong,[77a] A. Tiko,[77a] M. Tosi,[77a,77b] H. YARAR,[77a,77b] M. Zanetti,[77a,77b] P. Zotto,[77a,77b] A. Zucchetta,[77a,77b] G. Zumerle,[77a,77b] A. Braghieri,[78a] S. Calzaferri,[78a,78b] D. Fiorina,[78a,78b] P. Montagna,[78a,78b] S. P. Ratti,[78a,78b] V. Re,[78a] M. Ressegotti,[78a,78b] C. Riccardi,[78a,78b] P. Salvini,[78a] I. Vai,[78a] P. Vitulo,[78a,78b] M. Biasini,[79a,79b] G. M. Bilei,[79a] D. Ciangottini,[79a,79b] L. Fanò,[79a,79b] P. Lariccia,[79a,79b] G. Mantovani,[79a,79b] V. Mariani,[79a,79b] M. Menichelli,[79a] F. Moscatelli,[79a] A. Rossi,[79a,79b] A. Santocchia,[79a,79b] D. Spiga,[79a] T. Tedeschi,[79a,79b] K. Androsov,[80a] P. Azzurri,[80a] G. Bagliesi,[80a] V. Bertacchi,[80a,80c] L. Bianchini,[80a] T. Boccali,[80a] R. Castaldi,[80a] M. A. Ciocci,[80a,80b] R. Dell'Orso,[80a] M. R. Di Domenico,[80a,80b] S. Donato,[80a] L. Giannini,[80a,80c] A. Giassi,[80a] M. T. Grippo,[80a] F. Ligabue,[80a,80c] E. Manca,[80a,80c] G. Mandorli,[80a,80c] A. Messineo,[80a,80b] F. Palla,[80a] G. Ramirez-Sanchez,[80a,80c] A. Rizzi,[80a,80b] G. Rolandi,[80a,80c] S. Roy Chowdhury,[80a,80c] A. Scribano,[80a] N. Shafiei,[80a,80b] P. Spagnolo,[80a] R. Tenchini,[80a] G. Tonelli,[80a,80b] N. Turini,[80a] A. Venturi,[80a] P. G. Verdini,[80a] F. Cavallari,[81a] M. Cipriani,[81a,81b] D. Del Re,[81a,81b] E. Di Marco,[81a] M. Diemoz,[81a] E. Longo,[81a,81b] P. Meridiani,[81a] G. Organtini,[81a,81b] F. Pandolfi,[81a] R. Paramatti,[81a,81b] C. Quaranta,[81a,81b] S. Rahatlou,[81a,81b] C. Rovelli,[81a] F. Santanastasio,[81a,81b] L. Soffi,[81a,81b] R. Tramontano,[81a,81b] N. Amapane,[82a,82b] R. Arcidiacono,[82a,82c] S. Argiro,[82a,82b] M. Arneodo,[82a,82c] N. Bartosik,[82a] R. Bellan,[82a,82b] A. Bellora,[82a,82b] C. Biino,[82a] A. Cappati,[82a,82b] N. Cartiglia,[82a] S. Cometti,[82a] M. Costa,[82a,82b] R. Covarelli,[82a,82b] N. Demaria,[82a] B. Kiani,[82a,82b] F. Legger,[82a] C. Mariotti,[82a] S. Maselli,[82a] E. Migliore,[82a,82b] V. Monaco,[82a,82b] E. Monteil,[82a,82b] M. Monteno,[82a] M. M. Obertino,[82a,82b] G. Ortona,[82a] L. Pacher,[82a,82b] N. Pastrone,[82a] M. Pelliccioni,[82a] G. L. Pinna Angioni,[82a,82b] M. Ruspa,[82a,82c] R. Salvatico,[82a,82b] F. Siviero,[82a,82b] V. Sola,[82a] A. Solano,[82a,82b] D. Soldi,[82a,82b] A. Staiano,[82a] D. Trocino,[82a,82b] S. Belforte,[83a] V. Candelise,[83a,83b] M. Casarsa,[83a] F. Cossutti,[83a] A. Da Rold,[83a,83b] G. Della Ricca,[83a,83b] F. Vazzoler,[83a,83b] S. Dogra,[84] C. Huh,[84] B. Kim,[84] D. H. Kim,[84] G. N. Kim,[84] J. Lee,[84] S. W. Lee,[84] C. S. Moon,[84] Y. D. Oh,[84] S. I. Pak,[84] S. Sekmen,[84] Y. C. Yang,[84] H. Kim,[85] D. H. Moon,[85] B. Francois,[86] T. J. Kim,[86] J. Park,[86] S. Cho,[87] S. Choi,[87] Y. Go,[87] S. Ha,[87] B. Hong,[87] K. Lee,[87] K. S. Lee,[87] J. Lim,[87] J. Park,[87] S. K. Park,[87] J. Yoo,[87] J. Goh,[88] A. Gurtu,[88] H. S. Kim,[89] Y. Kim,[89] J. Almond,[90] J. H. Bhyun,[90] J. Choi,[90] S. Jeon,[90] J. Kim,[90] J. S. Kim,[90] S. Ko,[90] H. Kwon,[90] H. Lee,[90] K. Lee,[90] S. Lee,[90] K. Nam,[90] B. H. Oh,[90] M. Oh,[90] S. B. Oh,[90] B. C. Radburn-Smith,[90] H. Seo,[90] U. K. Yang,[90] I. Yoon,[90] D. Jeon,[91] J. H. Kim,[91] B. Ko,[91] J. S. H. Lee,[91] I. C. Park,[91] Y. Roh,[91] D. Song,[91] I. J. Watson,[91] H. D. Yoo,[92] Y. Choi,[93] C. Hwang,[93] Y. Jeong,[93] H. Lee,[93] J. Lee,[93] Y. Lee,[93] I. Yu,[93] Y. Maghrbi,[94] V. Veckalns,[95,pp] A. Juodagalvis,[96] A. Rinkevicius,[96] G. Tamulaitis,[96] W. A. T. Wan Abdullah,[97] M. N. Yusli,[97] Z. Zolkapli,[97] J. F. Benitez,[98] A. Castaneda Hernandez,[98] J. A. Murillo Quijada,[98] L. Valencia Palomo,[98] H. Castilla-Valdez,[99] E. De La Cruz-Burelo,[99] I. Heredia-De La Cruz,[99,qq] R. Lopez-Fernandez,[99] A. Sanchez-Hernandez,[99] S. Carrillo Moreno,[100] C. Oropeza Barrera,[100] M. Ramirez-Garcia,[100] F. Vazquez Valencia,[100] J. Eysermans,[101] I. Pedraza,[101] H. A. Salazar Ibarguen,[101] C. Uribe Estrada,[101] A. Morelos Pineda,[102] J. Mijuskovic,[103,e] N. Raicevic,[103] D. Krofcheck,[104] S. Bheesette,[105] P. H. Butler,[105] A. Ahmad,[106] M. I. Asghar,[106] M. I. M. Awan,[106] Q. Hassan,[106] H. R. Hoorani,[106] W. A. Khan,[106] M. A. Shah,[106] M. Shoaib,[106] M. Waqas,[106] V. Avati,[107] L. Grzanka,[107] M. Malawski,[107] H. Bialkowska,[108] M. Bluj,[108] B. Boimska,[108] T. Frueboes,[108] M. Górski,[108] M. Kazana,[108] M. Szleper,[108] P. Traczyk,[108] P. Zalewski,[108]

K. Bunkowski,[109] A. Byszuk,[109,rr] K. Doroba,[109] A. Kalinowski,[109] M. Konecki,[109] J. Krolikowski,[109] M. Olszewski,[109] M. Walczak,[109] M. Araujo,[110] P. Bargassa,[110] D. Bastos,[110] A. Di Francesco,[110] P. Faccioli,[110] B. Galinhas,[110] M. Gallinaro,[110] J. Hollar,[110] N. Leonardo,[110] T. Niknejad,[110] J. Seixas,[110] K. Shchelina,[110] O. Toldaiev,[110] J. Varela,[110] S. Afanasiev,[111] P. Bunin,[111] M. Gavrilenko,[111] I. Golutvin,[111] I. Gorbunov,[111] A. Kamenev,[111] V. Karjavine,[111] A. Lanev,[111] A. Malakhov,[111] V. Matveev,[111,ss,tt] P. Moisenz,[111] V. Palichik,[111] V. Perelygin,[111] M. Savina,[111] D. Seitova,[111] V. Shalaev,[111] S. Shmatov,[111] S. Shulha,[111] V. Smirnov,[111] O. Teryaev,[111] N. Voytishin,[111] A. Zarubin,[111] I. Zhizhin,[111] G. Gavrilov,[112] V. Golovtcov,[112] Y. Ivanov,[112] V. Kim,[112,uu] E. Kuznetsova,[112,vv] V. Murzin,[112] V. Oreshkin,[112] I. Smirnov,[112] D. Sosnov,[112] V. Sulimov,[112] L. Uvarov,[112] S. Volkov,[112] A. Vorobyev,[112] Yu. Andreev,[113] A. Dermenev,[113] S. Gninenko,[113] N. Golubev,[113] A. Karneyeu,[113] M. Kirsanov,[113] N. Krasnikov,[113] A. Pashenkov,[113] G. Pivovarov,[113] D. Tlisov,[113] A. Toropin,[113] V. Epshteyn,[114] V. Gavrilov,[114] N. Lychkovskaya,[114] A. Nikitenko,[114,ww] V. Popov,[114] I. Pozdnyakov,[114] G. Safronov,[114] A. Spiridonov,[114] A. Stepennov,[114] M. Toms,[114] E. Vlasov,[114] A. Zhokin,[114] T. Aushev,[115] M. Chadeeva,[116,xx] A. Oskin,[116] P. Parygin,[116] E. Popova,[116] V. Rusinov,[116] V. Andreev,[117] M. Azarkin,[117] I. Dremin,[117] M. Kirakosyan,[117] A. Terkulov,[117] A. Baskakov,[118] A. Belyaev,[118] E. Boos,[118] V. Bunichev,[118] M. Dubinin,[118,yy] L. Dudko,[118] V. Klyukhin,[118] O. Kodolova,[118] I. Lokhtin,[118] S. Obraztsov,[118] M. Perfilov,[118] V. Savrin,[118] A. Snigirev,[118] V. Blinov,[119,zz] T. Dimova,[119,zz] L. Kardapoltsev,[119,zz] I. Ovtin,[119,zz] Y. Skovpen,[119,zz] I. Azhgirey,[120] I. Bayshev,[120] V. Kachanov,[120] A. Kalinin,[120] D. Konstantinov,[120] V. Petrov,[120] R. Ryutin,[120] A. Sobol,[120] S. Troshin,[120] N. Tyurin,[120] A. Uzunian,[120] A. Volkov,[120] A. Babaev,[121] A. Iuzhakov,[121] V. Okhotnikov,[121] L. Sukhikh,[121] V. Borchsh,[122] V. Ivanchenko,[122] E. Tcherniaev,[122] P. Adzic,[123,aaa] P. Cirkovic,[123] M. Dordevic,[123] P. Milenovic,[123] J. Milosevic,[123] M. Aguilar-Benitez,[124] J. Alcaraz Maestre,[124] A. Álvarez Fernández,[124] I. Bachiller,[124] M. Barrio Luna,[124] C. F. Bedoya,[124] J. A. Brochero Cifuentes,[124] C. A. Carrillo Montoya,[124] M. Cepeda,[124] M. Cerrada,[124] N. Colino,[124] B. De La Cruz,[124] A. Delgado Peris,[124] J. P. Fernández Ramos,[124] J. Flix,[124] M. C. Fouz,[124] O. Gonzalez Lopez,[124] S. Goy Lopez,[124] J. M. Hernandez,[124] M. I. Josa,[124] D. Moran,[124] Á. Navarro Tobar,[124] A. Pérez-Calero Yzquierdo,[124] J. Puerta Pelayo,[124] I. Redondo,[124] L. Romero,[124] S. Sánchez Navas,[124] M. S. Soares,[124] A. Triossi,[124] C. Willmott,[124] C. Albajar,[125] J. F. de Trocóniz,[125] R. Reyes-Almanza,[125] B. Alvarez Gonzalez,[126] J. Cuevas,[126] C. Erice,[126] J. Fernandez Menendez,[126] S. Folgueras,[126] I. Gonzalez Caballero,[126] E. Palencia Cortezon,[126] C. Ramón Álvarez,[126] V. Rodríguez Bouza,[126] S. Sanchez Cruz,[126] I. J. Cabrillo,[127] A. Calderon,[127] B. Chazin Quero,[127] J. Duarte Campderros,[127] M. Fernandez,[127] P. J. Fernández Manteca,[127] A. García Alonso,[127] G. Gomez,[127] C. Martinez Rivero,[127] P. Martinez Ruiz del Arbol,[127] F. Matorras,[127] J. Piedra Gomez,[127] C. Prieels,[127] F. Ricci-Tam,[127] T. Rodrigo,[127] A. Ruiz-Jimeno,[127] L. Russo,[127,bbb] L. Scodellaro,[127] I. Vila,[127] J. M. Vizan Garcia,[127] MK Jayananda,[128] B. Kailasapathy,[128,ccc] D. U. J. Sonnadara,[128] DDC Wickramarathna,[128] W. G. D. Dharmaratna,[129] K. Liyanage,[129] N. Perera,[129] N. Wickramage,[129] T. K. Aarrestad,[130] D. Abbaneo,[130] B. Akgun,[130] E. Auffray,[130] G. Auzinger,[130] J. Baechler,[130] P. Baillon,[130] A. H. Ball,[130] D. Barney,[130] J. Bendavid,[130] N. Beni,[130] M. Bianco,[130] A. Bocci,[130] P. Bortignon,[130] E. Bossini,[130] E. Brondolin,[130] T. Camporesi,[130] G. Cerminara,[130] L. Cristella,[130] D. d'Enterria,[130] A. Dabrowski,[130] N. Daci,[130] V. Daponte,[130] A. David,[130] A. De Roeck,[130] M. Deile,[130] R. Di Maria,[130] M. Dobson,[130] M. Dünser,[130] N. Dupont,[130] A. Elliott-Peisert,[130] N. Emriskova,[130] F. Fallavollita,[130,ddd] D. Fasanella,[130] S. Fiorendi,[130] G. Franzoni,[130] J. Fulcher,[130] W. Funk,[130] S. Giani,[130] D. Gigi,[130] K. Gill,[130] F. Glege,[130] L. Gouskos,[130] M. Guilbaud,[130] D. Gulhan,[130] M. Haranko,[130] J. Hegeman,[130] Y. Iiyama,[130] V. Innocente,[130] T. James,[130] P. Janot,[130] J. Kaspar,[130] J. Kieseler,[130] M. Komm,[130] N. Kratochwil,[130] C. Lange,[130] P. Lecoq,[130] K. Long,[130] C. Lourenço,[130] L. Malgeri,[130] M. Mannelli,[130] A. Massironi,[130] F. Meijers,[130] S. Mersi,[130] E. Meschi,[130] F. Moortgat,[130] M. Mulders,[130] J. Ngadiuba,[130] J. Niedziela,[130] S. Orfanelli,[130] L. Orsini,[130] F. Pantaleo,[130,t] L. Pape,[130] E. Perez,[130] M. Peruzzi,[130] A. Petrilli,[130] G. Petrucciani,[130] A. Pfeiffer,[130] M. Pierini,[130] D. Rabady,[130] A. Racz,[130] M. Rieger,[130] M. Rovere,[130] H. Sakulin,[130] J. Salfeld-Nebgen,[130] S. Scarfi,[130] C. Schäfer,[130] C. Schwick,[130] M. Selvaggi,[130] A. Sharma,[130] P. Silva,[130] W. Snoeys,[130] P. Sphicas,[130,eee] J. Steggemann,[130] S. Summers,[130] V. R. Tavolaro,[130] D. Treille,[130] A. Tsirou,[130] G. P. Van Onsem,[130] A. Vartak,[130] M. Verzetti,[130] K. A. Wozniak,[130] W. D. Zeuner,[130] L. Caminada,[131,fff] W. Erdmann,[131] R. Horisberger,[131] Q. Ingram,[131] H. C. Kaestli,[131] D. Kotlinski,[131] U. Langenegger,[131] T. Rohe,[131] M. Backhaus,[132] P. Berger,[132] A. Calandri,[132] N. Chernyavskaya,[132] G. Dissertori,[132] M. Dittmar,[132] M. Donegà,[132] C. Dorfer,[132] T. Gadek,[132] T. A. Gómez Espinosa,[132] C. Grab,[132] D. Hits,[132] W. Lustermann,[132] A.-M. Lyon,[132] R. A. Manzoni,[132] M. T. Meinhard,[132] F. Micheli,[132] P. Musella,[132] F. Nessi-Tedaldi,[132] F. Pauss,[132] V. Perovic,[132] G. Perrin,[132] L. Perrozzi,[132] S. Pigazzini,[132] M. G. Ratti,[132] M. Reichmann,[132] C. Reissel,[132] T. Reitenspiess,[132] B. Ristic,[132] D. Ruini,[132] D. A. Sanz Becerra,[132] M. Schönenberger,[132] L. Shchutska,[132] V. Stampf,[132] M. L. Vesterbacka Olsson,[132]

R. Wallny,[132] D. H. Zhu,[132] C. Amsler,[133,ggg] C. Botta,[133] D. Brzhechko,[133] M. F. Canelli,[133] A. De Cosa,[133] R. Del Burgo,[133] J. K. Heikkilä,[133] M. Huwiler,[133] A. Jofrehei,[133] B. Kilminster,[133] S. Leontsinis,[133] A. Macchiolo,[133] P. Meiring,[133] V. M. Mikuni,[133] U. Molinatti,[133] I. Neutelings,[133] G. Rauco,[133] A. Reimers,[133] P. Robmann,[133] K. Schweiger,[133] Y. Takahashi,[133] S. Wertz,[133] C. Adloff,[134,hhh] C. M. Kuo,[134] W. Lin,[134] A. Roy,[134] T. Sarkar,[134,ii] S. S. Yu,[134] L. Ceard,[135] P. Chang,[135] Y. Chao,[135] K. F. Chen,[135] P. H. Chen,[135] W.-S. Hou,[135] Y. y. Li,[135] R.-S. Lu,[135] E. Paganis,[135] A. Psallidas,[135] A. Steen,[135] E. Yazgan,[135] B. Asavapibhop,[136] C. Asawatangtrakuldee,[136] N. Srimanobhas,[136] F. Boran,[137] S. Damarseckin,[137,iii] Z. S. Demiroglu,[137] F. Dolek,[137] C. Dozen,[137,jjj] I. Dumanoglu,[137,kkk] E. Eskut,[137] G. Gokbulut,[137] Y. Guler,[137] E. Gurpinar Guler,[137,lll] I. Hos,[137,mmm] C. Isik,[137] E. E. Kangal,[137,nnn] O. Kara,[137] A. Kayis Topaksu,[137] U. Kiminsu,[137] G. Onengut,[137] K. Ozdemir,[137,ooo] A. Polatoz,[137] A. E. Simsek,[137] B. Tali,[137,ppp] U. G. Tok,[137] S. Turkcapar,[137] I. S. Zorbakir,[137] C. Zorbilmez,[137] B. Isildak,[138,qqq] G. Karapinar,[138,rrr] K. Ocalan,[138,sss] M. Yalvac,[138,ttt] I. O. Atakisi,[139] E. Gülmez,[139] M. Kaya,[139,uuu] O. Kaya,[139,vvv] Ö. Özçelik,[139] S. Tekten,[139,www] E. A. Yetkin,[139,xxx] A. Cakir,[140] K. Cankocak,[140,kkk] Y. Komurcu,[140] S. Sen,[140,yyy] F. Aydogmus Sen,[141] S. Cerci,[141,ppp] B. Kaynak,[141] S. Ozkorucuklu,[141] D. Sunar Cerci,[141,ppp] B. Grynyov,[142] L. Levchuk,[143] E. Bhal,[144] S. Bologna,[144] J. J. Brooke,[144] D. Burns,[144,zzz] E. Clement,[144] D. Cussans,[144] H. Flacher,[144] J. Goldstein,[144] G. P. Heath,[144] H. F. Heath,[144] L. Kreczko,[144] B. Krikler,[144] S. Paramesvaran,[144] T. Sakuma,[144] S. Seif El Nasr-Storey,[144] V. J. Smith,[144] J. Taylor,[144] A. Titterton,[144] K. W. Bell,[145] A. Belyaev,[145,aaaa] C. Brew,[145] R. M. Brown,[145] D. J. A. Cockerill,[145] K. V. Ellis,[145] K. Harder,[145] S. Harper,[145] J. Linacre,[145] K. Manolopoulos,[145] D. M. Newbold,[145] E. Olaiya,[145] D. Petyt,[145] T. Reis,[145] T. Schuh,[145] C. H. Shepherd-Themistocleous,[145] A. Thea,[145] I. R. Tomalin,[145] T. Williams,[145] R. Bainbridge,[146] P. Bloch,[146] S. Bonomally,[146] J. Borg,[146] S. Breeze,[146] O. Buchmuller,[146] A. Bundock,[146] V. Cepaitis,[146] G. S. Chahal,[146,bbbb] D. Colling,[146] P. Dauncey,[146] G. Davies,[146] M. Della Negra,[146] P. Everaerts,[146] G. Fedi,[146] G. Hall,[146] G. Iles,[146] J. Langford,[146] L. Lyons,[146] A.-M. Magnan,[146] S. Malik,[146] A. Martelli,[146] V. Milosevic,[146] J. Nash,[146,cccc] V. Palladino,[146] M. Pesaresi,[146] D. M. Raymond,[146] A. Richards,[146] A. Rose,[146] E. Scott,[146] C. Seez,[146] A. Shtipliyski,[146] M. Stoye,[146] A. Tapper,[146] K. Uchida,[146] T. Virdee,[146,t] N. Wardle,[146] S. N. Webb,[146] D. Winterbottom,[146] A. G. Zecchinelli,[146] S. C. Zenz,[146] J. E. Cole,[147] P. R. Hobson,[147] A. Khan,[147] P. Kyberd,[147] C. K. Mackay,[147] I. D. Reid,[147] L. Teodorescu,[147] S. Zahid,[147] A. Brinkerhoff,[148] K. Call,[148] B. Caraway,[148] J. Dittmann,[148] K. Hatakeyama,[148] A. R. Kanuganti,[148] C. Madrid,[148] B. McMaster,[148] N. Pastika,[148] S. Sawant,[148] C. Smith,[148] R. Bartek,[149] A. Dominguez,[149] R. Uniyal,[149] A. M. Vargas Hernandez,[149] A. Buccilli,[150] O. Charaf,[150] S. I. Cooper,[150] S. V. Gleyzer,[150] C. Henderson,[150] P. Rumerio,[150] C. West,[150] A. Akpinar,[151] A. Albert,[151] D. Arcaro,[151] C. Cosby,[151] Z. Demiragli,[151] D. Gastler,[151] C. Richardson,[151] J. Rohlf,[151] K. Salyer,[151] D. Sperka,[151] D. Spitzbart,[151] I. Suarez,[151] S. Yuan,[151] D. Zou,[151] G. Benelli,[152] B. Burkle,[152] X. Coubez,[152,u] D. Cutts,[152] Y. t. Duh,[152] M. Hadley,[152] U. Heintz,[152] J. M. Hogan,[152,dddd] K. H. M. Kwok,[152] E. Laird,[152] G. Landsberg,[152] K. T. Lau,[152] J. Lee,[152] M. Narain,[152] S. Sagir,[152,eeee] R. Syarif,[152] E. Usai,[152] W. Y. Wong,[152] D. Yu,[152] W. Zhang,[152] R. Band,[153] C. Brainerd,[153] R. Breedon,[153] M. Calderon De La Barca Sanchez,[153] M. Chertok,[153] J. Conway,[153] R. Conway,[153] P. T. Cox,[153] R. Erbacher,[153] C. Flores,[153] G. Funk,[153] F. Jensen,[153] W. Ko,[153,a] O. Kukral,[153] R. Lander,[153] M. Mulhearn,[153] D. Pellett,[153] J. Pilot,[153] M. Shi,[153] D. Taylor,[153] K. Tos,[153] M. Tripathi,[153] Y. Yao,[153] F. Zhang,[153] M. Bachtis,[154] C. Bravo,[154] R. Cousins,[154] A. Dasgupta,[154] A. Florent,[154] D. Hamilton,[154] J. Hauser,[154] M. Ignatenko,[154] T. Lam,[154] N. Mccoll,[154] W. A. Nash,[154] S. Regnard,[154] D. Saltzberg,[154] C. Schnaible,[154] B. Stone,[154] V. Valuev,[154] K. Burt,[155] Y. Chen,[155] R. Clare,[155] J. W. Gary,[155] S. M. A. Ghiasi Shirazi,[155] G. Hanson,[155] G. Karapostoli,[155] O. R. Long,[155] N. Manganelli,[155] M. Olmedo Negrete,[155] M. I. Paneva,[155] W. Si,[155] S. Wimpenny,[155] Y. Zhang,[155] J. G. Branson,[156] P. Chang,[156] S. Cittolin,[156] S. Cooperstein,[156] N. Deelen,[156] M. Derdzinski,[156] J. Duarte,[156] R. Gerosa,[156] D. Gilbert,[156] B. Hashemi,[156] D. Klein,[156] V. Krutelyov,[156] J. Letts,[156] M. Masciovecchio,[156] S. May,[156] S. Padhi,[156] M. Pieri,[156] V. Sharma,[156] M. Tadel,[156] F. Würthwein,[156] A. Yagil,[156] N. Amin,[157] R. Bhandari,[157] C. Campagnari,[157] M. Citron,[157] A. Dorsett,[157] V. Dutta,[157] J. Incandela,[157] B. Marsh,[157] H. Mei,[157] A. Ovcharova,[157] H. Qu,[157] M. Quinnan,[157] J. Richman,[157] U. Sarica,[157] D. Stuart,[157] S. Wang,[157] D. Anderson,[158] A. Bornheim,[158] O. Cerri,[158] I. Dutta,[158] J. M. Lawhorn,[158] N. Lu,[158] J. Mao,[158] H. B. Newman,[158] T. Q. Nguyen,[158] J. Pata,[158] M. Spiropulu,[158] J. R. Vlimant,[158] S. Xie,[158] Z. Zhang,[158] R. Y. Zhu,[158] J. Alison,[159] M. B. Andrews,[159] T. Ferguson,[159] T. Mudholkar,[159] M. Paulini,[159] M. Sun,[159] I. Vorobiev,[159] M. Weinberg,[159] J. P. Cumalat,[160] W. T. Ford,[160] E. MacDonald,[160] T. Mulholland,[160] R. Patel,[160] A. Perloff,[160] K. Stenson,[160] K. A. Ulmer,[160] S. R. Wagner,[160] J. Alexander,[161] Y. Cheng,[161] J. Chu,[161] D. J. Cranshaw,[161] A. Datta,[161] A. Frankenthal,[161] K. Mcdermott,[161] J. Monroy,[161] J. R. Patterson,[161] D. Quach,[161] A. Ryd,[161] W. Sun,[161] S. M. Tan,[161] Z. Tao,[161] J. Thom,[161] P. Wittich,[161] M. Zientek,[161] S. Abdullin,[162] M. Albrow,[162] M. Alyari,[162] G. Apollinari,[162]

A. Apresyan,[162] A. Apyan,[162] S. Banerjee,[162] L. A. T. Bauerdick,[162] A. Beretvas,[162] D. Berry,[162] J. Berryhill,[162] P. C. Bhat,[162] K. Burkett,[162] J. N. Butler,[162] A. Canepa,[162] G. B. Cerati,[162] H. W. K. Cheung,[162] F. Chlebana,[162] M. Cremonesi,[162] V. D. Elvira,[162] J. Freeman,[162] Z. Gecse,[162] E. Gottschalk,[162] L. Gray,[162] D. Green,[162] S. Grünendahl,[162] O. Gutsche,[162] R. M. Harris,[162] S. Hasegawa,[162] R. Heller,[162] T. C. Herwig,[162] J. Hirschauer,[162] B. Jayatilaka,[162] S. Jindariani,[162] M. Johnson,[162] U. Joshi,[162] T. Klijnsma,[162] B. Klima,[162] M. J. Kortelainen,[162] S. Lammel,[162] J. Lewis,[162] D. Lincoln,[162] R. Lipton,[162] M. Liu,[162] T. Liu,[162] J. Lykken,[162] K. Maeshima,[162] D. Mason,[162] P. McBride,[162] P. Merkel,[162] S. Mrenna,[162] S. Nahn,[162] V. O'Dell,[162] V. Papadimitriou,[162] K. Pedro,[162] C. Pena,[162,yy] O. Prokofyev,[162] F. Ravera,[162] A. Reinsvold Hall,[162] L. Ristori,[162] B. Schneider,[162] E. Sexton-Kennedy,[162] N. Smith,[162] A. Soha,[162] W. J. Spalding,[162] L. Spiegel,[162] S. Stoynev,[162] J. Strait,[162] L. Taylor,[162] S. Tkaczyk,[162] N. V. Tran,[162] L. Uplegger,[162] E. W. Vaandering,[162] M. Wang,[162] H. A. Weber,[162] A. Woodard,[162] D. Acosta,[163] P. Avery,[163] D. Bourilkov,[163] L. Cadamuro,[163] V. Cherepanov,[163] F. Errico,[163] R. D. Field,[163] D. Guerrero,[163] B. M. Joshi,[163] M. Kim,[163] J. Konigsberg,[163] A. Korytov,[163] K. H. Lo,[163] K. Matchev,[163] N. Menendez,[163] G. Mitselmakher,[163] D. Rosenzweig,[163] K. Shi,[163] J. Wang,[163] S. Wang,[163] X. Zuo,[163] Y. R. Joshi,[164] T. Adams,[165] A. Askew,[165] D. Diaz,[165] R. Habibullah,[165] S. Hagopian,[165] V. Hagopian,[165] K. F. Johnson,[165] R. Khurana,[165] T. Kolberg,[165] G. Martinez,[165] H. Prosper,[165] C. Schiber,[165] R. Yohay,[165] J. Zhang,[165] M. M. Baarmand,[166] S. Butalla,[166] T. Elkafrawy,[166,o] M. Hohlmann,[166] D. Noonan,[166] M. Rahmani,[166] M. Saunders,[166] F. Yumiceva,[166] M. R. Adams,[167] L. Apanasevich,[167] H. Becerril Gonzalez,[167] R. Cavanaugh,[167] X. Chen,[167] S. Dittmer,[167] O. Evdokimov,[167] C. E. Gerber,[167] D. A. Hangal,[167] D. J. Hofman,[167] C. Mills,[167] G. Oh,[167] T. Roy,[167] M. B. Tonjes,[167] N. Varelas,[167] J. Viinikainen,[167] H. Wang,[167] X. Wang,[167] Z. Wu,[167] M. Alhusseini,[168] B. Bilki,[168,lll] K. Dilsiz,[168,ffff] S. Durgut,[168] R. P. Gandrajula,[168] M. Haytmyradov,[168] V. Khristenko,[168] O. K. Köseyan,[168] J.-P. Merlo,[168] A. Mestvirishvili,[168,gggg] A. Moeller,[168] J. Nachtman,[168] H. Ogul,[168,hhhh] Y. Onel,[168] F. Ozok,[168,iiii] A. Penzo,[168] C. Snyder,[168] E. Tiras,[168] J. Wetzel,[168] K. Yi,[168,jjjj] O. Amram,[169] B. Blumenfeld,[169] L. Corcodilos,[169] M. Eminizer,[169] A. V. Gritsan,[169] S. Kyriacou,[169] P. Maksimovic,[169] C. Mantilla,[169] J. Roskes,[169] M. Swartz,[169] T. Á. Vámi,[169] C. Baldenegro Barrera,[170] P. Baringer,[170] A. Bean,[170] A. Bylinkin,[170] T. Isidori,[170] S. Khalil,[170] J. King,[170] G. Krintiras,[170] A. Kropivnitskaya,[170] C. Lindsey,[170] N. Minafra,[170] M. Murray,[170] C. Rogan,[170] C. Royon,[170] S. Sanders,[170] E. Schmitz,[170] J. D. Tapia Takaki,[170] Q. Wang,[170] J. Williams,[170] G. Wilson,[170] S. Duric,[171] A. Ivanov,[171] K. Kaadze,[171] D. Kim,[171] Y. Maravin,[171] D. R. Mendis,[171] T. Mitchell,[171] A. Modak,[171] A. Mohammadi,[171] F. Rebassoo,[172] D. Wright,[172] E. Adams,[173] A. Baden,[173] O. Baron,[173] A. Belloni,[173] S. C. Eno,[173] Y. Feng,[173] N. J. Hadley,[173] S. Jabeen,[173] G. Y. Jeng,[173] R. G. Kellogg,[173] T. Koeth,[173] A. C. Mignerey,[173] S. Nabili,[173] M. Seidel,[173] A. Skuja,[173] S. C. Tonwar,[173] L. Wang,[173] K. Wong,[173] D. Abercrombie,[174] B. Allen,[174] R. Bi,[174] S. Brandt,[174] W. Busza,[174] I. A. Cali,[174] Y. Chen,[174] M. D'Alfonso,[174] G. Gomez Ceballos,[174] M. Goncharov,[174] P. Harris,[174] D. Hsu,[174] M. Hu,[174] M. Klute,[174] D. Kovalskyi,[174] J. Krupa,[174] Y.-J. Lee,[174] P. D. Luckey,[174] B. Maier,[174] A. C. Marini,[174] C. Mcginn,[174] C. Mironov,[174] S. Narayanan,[174] X. Niu,[174] C. Paus,[174] D. Rankin,[174] C. Roland,[174] G. Roland,[174] Z. Shi,[174] G. S. F. Stephans,[174] K. Sumorok,[174] K. Tatar,[174] D. Velicanu,[174] J. Wang,[174] T. W. Wang,[174] Z. Wang,[174] B. Wyslouch,[174] R. M. Chatterjee,[175] A. Evans,[175] S. Guts,[175,a] P. Hansen,[175] J. Hiltbrand,[175] Sh. Jain,[175] M. Krohn,[175] Y. Kubota,[175] Z. Lesko,[175] J. Mans,[175] M. Revering,[175] R. Rusack,[175] R. Saradhy,[175] N. Schroeder,[175] N. Strobbe,[175] M. A. Wadud,[175] J. G. Acosta,[176] S. Oliveros,[176] K. Bloom,[177] S. Chauhan,[177] D. R. Claes,[177] C. Fangmeier,[177] L. Finco,[177] F. Golf,[177] J. R. González Fernández,[177] I. Kravchenko,[177] J. E. Siado,[177] G. R. Snow,[177,a] B. Stieger,[177] W. Tabb,[177] G. Agarwal,[178] C. Harrington,[178] L. Hay,[178] I. Iashvili,[178] A. Kharchilava,[178] C. McLean,[178] D. Nguyen,[178] A. Parker,[178] J. Pekkanen,[178] S. Rappoccio,[178] B. Roozbahani,[178] G. Alverson,[179] E. Barberis,[179] C. Freer,[179] Y. Haddad,[179] A. Hortiangtham,[179] G. Madigan,[179] B. Marzocchi,[179] D. M. Morse,[179] V. Nguyen,[179] T. Orimoto,[179] L. Skinnari,[179] A. Tishelman-Charny,[179] T. Wamorkar,[179] B. Wang,[179] A. Wisecarver,[179] D. Wood,[179] S. Bhattacharya,[180] J. Bueghly,[180] Z. Chen,[180] A. Gilbert,[180] T. Gunter,[180] K. A. Hahn,[180] N. Odell,[180] M. H. Schmitt,[180] K. Sung,[180] M. Velasco,[180] R. Bucci,[181] N. Dev,[181] R. Goldouzian,[181] M. Hildreth,[181] K. Hurtado Anampa,[181] C. Jessop,[181] D. J. Karmgard,[181] K. Lannon,[181] W. Li,[181] N. Loukas,[181] N. Marinelli,[181] I. Mcalister,[181] F. Meng,[181] K. Mohrman,[181] Y. Musienko,[181,ss] R. Ruchti,[181] P. Siddireddy,[181] S. Taroni,[181] M. Wayne,[181] A. Wightman,[181] M. Wolf,[181] L. Zygala,[181] J. Alimena,[182] B. Bylsma,[182] B. Cardwell,[182] L. S. Durkin,[182] B. Francis,[182] C. Hill,[182] W. Ji,[182] A. Lefeld,[182] B. L. Winer,[182] B. R. Yates,[182] G. Dezoort,[183] P. Elmer,[183] B. Greenberg,[183] N. Haubrich,[183] S. Higginbotham,[183] A. Kalogeropoulos,[183] G. Kopp,[183] S. Kwan,[183] D. Lange,[183] M. T. Lucchini,[183] J. Luo,[183] D. Marlow,[183] K. Mei,[183] I. Ojalvo,[183] J. Olsen,[183] C. Palmer,[183] P. Piroué,[183] D. Stickland,[183] C. Tully,[183] S. Malik,[184] S. Norberg,[184] V. E. Barnes,[185] R. Chawla,[185] S. Das,[185] L. Gutay,[185] M. Jones,[185] A. W. Jung,[185] B. Mahakud,[185] G. Negro,[185] N. Neumeister,[185] C. C. Peng,[185] S. Piperov,[185]

H. Qiu,[185] J. F. Schulte,[185] N. Trevisani,[185] F. Wang,[185] R. Xiao,[185] W. Xie,[185] T. Cheng,[186] J. Dolen,[186] N. Parashar,[186] M. Stojanovic,[186] A. Baty,[187] S. Dildick,[187] K. M. Ecklund,[187] S. Freed,[187] F. J. M. Geurts,[187] M. Kilpatrick,[187] A. Kumar,[187] W. Li,[187] B. P. Padley,[187] R. Redjimi,[187] J. Roberts,[187,a] J. Rorie,[187] W. Shi,[187] A. G. Stahl Leiton,[187] Z. Tu,[187] A. Zhang,[187] A. Bodek,[188] P. de Barbaro,[188] R. Demina,[188] J. L. Dulemba,[188] C. Fallon,[188] T. Ferbel,[188] M. Galanti,[188] A. Garcia-Bellido,[188] O. Hindrichs,[188] A. Khukhunaishvili,[188] E. Ranken,[188] R. Taus,[188] B. Chiarito,[189] J. P. Chou,[189] A. Gandrakota,[189] Y. Gershtein,[189] E. Halkiadakis,[189] A. Hart,[189] M. Heindl,[189] E. Hughes,[189] S. Kaplan,[189] O. Karacheban,[189,x] I. Laflotte,[189] A. Lath,[189] R. Montalvo,[189] K. Nash,[189] M. Osherson,[189] S. Salur,[189] S. Schnetzer,[189] S. Somalwar,[189] R. Stone,[189] S. A. Thayil,[189] S. Thomas,[189] H. Acharya,[190] A. G. Delannoy,[190] S. Spanier,[190] O. Bouhali,[191,kkkk] M. Dalchenko,[191] A. Delgado,[191] R. Eusebi,[191] J. Gilmore,[191] T. Huang,[191] T. Kamon,[191,llll] H. Kim,[191] S. Luo,[191] S. Malhotra,[191] R. Mueller,[191] D. Overton,[191] L. Perniè,[191] D. Rathjens,[191] A. Safonov,[191] N. Akchurin,[192] J. Damgov,[192] V. Hegde,[192] S. Kunori,[192] K. Lamichhane,[192] S. W. Lee,[192] T. Mengke,[192] S. Muthumuni,[192] T. Peltola,[192] S. Undleeb,[192] I. Volobouev,[192] Z. Wang,[192] A. Whitbeck,[192] E. Appelt,[193] S. Greene,[193] A. Gurrola,[193] R. Janjam,[193] W. Johns,[193] C. Maguire,[193] A. Melo,[193] H. Ni,[193] K. Padeken,[193] F. Romeo,[193] P. Sheldon,[193] S. Tuo,[193] J. Velkovska,[193] M. Verweij,[193] L. Ang,[194] M. W. Arenton,[194] B. Cox,[194] G. Cummings,[194] J. Hakala,[194] R. Hirosky,[194] M. Joyce,[194] A. Ledovskoy,[194] C. Neu,[194] B. Tannenwald,[194] Y. Wang,[194] E. Wolfe,[194] F. Xia,[194] P. E. Karchin,[195] N. Poudyal,[195] J. Sturdy,[195] P. Thapa,[195] K. Black,[196] T. Bose,[196] J. Buchanan,[196] C. Caillol,[196] S. Dasu,[196] I. De Bruyn,[196] L. Dodd,[196] C. Galloni,[196] H. He,[196] M. Herndon,[196] A. Hervé,[196] U. Hussain,[196] A. Lanaro,[196] A. Loeliger,[196] R. Loveless,[196] J. Madhusudanan Sreekala,[196] A. Mallampalli,[196] D. Pinna,[196] T. Ruggles,[196] A. Savin,[196] V. Shang,[196] V. Sharma,[196] W. H. Smith,[196] D. Teague,[196] S. Trembath-reichert,[196] and W. Vetens[196]

(CMS Collaboration)

[1]*Yerevan Physics Institute, Yerevan, Armenia*
[2]*Institut für Hochenergiephysik, Wien, Austria*
[3]*Institute for Nuclear Problems, Minsk, Belarus*
[4]*Universiteit Antwerpen, Antwerpen, Belgium*
[5]*Vrije Universiteit Brussel, Brussel, Belgium*
[6]*Université Libre de Bruxelles, Bruxelles, Belgium*
[7]*Ghent University, Ghent, Belgium*
[8]*Université Catholique de Louvain, Louvain-la-Neuve, Belgium*
[9]*Centro Brasileiro de Pesquisas Fisicas, Rio de Janeiro, Brazil*
[10]*Universidade do Estado do Rio de Janeiro, Rio de Janeiro, Brazil*
[11a]*Universidade Estadual Paulista, São Paulo, Brazil*
[11b]*Universidade Federal do ABC, São Paulo, Brazil*
[12]*Institute for Nuclear Research and Nuclear Energy, Bulgarian Academy of Sciences, Sofia, Bulgaria*
[13]*University of Sofia, Sofia, Bulgaria*
[14]*Beihang University, Beijing, China*
[15]*Department of Physics, Tsinghua University, Beijing, China*
[16]*Institute of High Energy Physics, Beijing, China*
[17]*State Key Laboratory of Nuclear Physics and Technology, Peking University, Beijing, China*
[18]*Sun Yat-Sen University, Guangzhou, China*
[19]*Institute of Modern Physics and Key Laboratory of Nuclear Physics and Ion-beam Application (MOE)—Fudan University, Shanghai, China*
[20]*Zhejiang University, Hangzhou, China*
[21]*Universidad de Los Andes, Bogota, Colombia*
[22]*Universidad de Antioquia, Medellin, Colombia*
[23]*University of Split, Faculty of Electrical Engineering, Mechanical Engineering and Naval Architecture, Split, Croatia*
[24]*University of Split, Faculty of Science, Split, Croatia*
[25]*Institute Rudjer Boskovic, Zagreb, Croatia*
[26]*University of Cyprus, Nicosia, Cyprus*
[27]*Charles University, Prague, Czech Republic*
[28]*Escuela Politecnica Nacional, Quito, Ecuador*
[29]*Universidad San Francisco de Quito, Quito, Ecuador*

[30]Academy of Scientific Research and Technology of the Arab Republic of Egypt,
Egyptian Network of High Energy Physics, Cairo, Egypt

[31]Center for High Energy Physics (CHEP-FU), Fayoum University, El-Fayoum, Egypt

[32]National Institute of Chemical Physics and Biophysics, Tallinn, Estonia

[33]Department of Physics, University of Helsinki, Helsinki, Finland

[34]Helsinki Institute of Physics, Helsinki, Finland

[35]Lappeenranta University of Technology, Lappeenranta, Finland

[36]IRFU, CEA, Université Paris-Saclay, Gif-sur-Yvette, France

[37]Laboratoire Leprince-Ringuet, CNRS/IN2P3, Ecole Polytechnique, Institut Polytechnique de Paris,
Paris, France

[38]Université de Strasbourg, CNRS, IPHC UMR 7178, Strasbourg, France

[39]Université de Lyon, Université Claude Bernard Lyon 1, CNRS-IN2P3,
Institut de Physique Nucléaire de Lyon, Villeurbanne, France

[40]Georgian Technical University, Tbilisi, Georgia

[41]RWTH Aachen University, I. Physikalisches Institut, Aachen, Germany

[42]RWTH Aachen University, III. Physikalisches Institut A, Aachen, Germany

[43]RWTH Aachen University, III. Physikalisches Institut B, Aachen, Germany

[44]Deutsches Elektronen-Synchrotron, Hamburg, Germany

[45]University of Hamburg, Hamburg, Germany

[46]Karlsruher Institut fuer Technologie, Karlsruhe, Germany

[47]Institute of Nuclear and Particle Physics (INPP), NCSR Demokritos, Aghia Paraskevi, Greece

[48]National and Kapodistrian University of Athens, Athens, Greece

[49]National Technical University of Athens, Athens, Greece

[50]University of Ioánnina, Ioánnina, Greece

[51]MTA-ELTE Lendület CMS Particle and Nuclear Physics Group, Eötvös Loránd University,
Budapest, Hungary

[52]Wigner Research Centre for Physics, Budapest, Hungary

[53]Institute of Nuclear Research ATOMKI, Debrecen, Hungary

[54]Institute of Physics, University of Debrecen, Debrecen, Hungary

[55]Eszterhazy Karoly University, Karoly Robert Campus, Gyongyos, Hungary

[56]Indian Institute of Science (IISc), Bangalore, India

[57]National Institute of Science Education and Research, HBNI, Bhubaneswar, India

[58]Panjab University, Chandigarh, India

[59]University of Delhi, Delhi, India

[60]Saha Institute of Nuclear Physics, HBNI, Kolkata, India

[61]Indian Institute of Technology Madras, Madras, India

[62]Bhabha Atomic Research Centre, Mumbai, India

[63]Tata Institute of Fundamental Research-A, Mumbai, India

[64]Tata Institute of Fundamental Research-B, Mumbai, India

[65]Indian Institute of Science Education and Research (IISER), Pune, India

[66]Department of Physics, Isfahan University of Technology, Isfahan, Iran

[67]Institute for Research in Fundamental Sciences (IPM), Tehran, Iran

[68]University College Dublin, Dublin, Ireland

[69a]INFN Sezione di Bari, Bari, Italy

[69b]Università di Bari, Bari, Italy

[69c]Politecnico di Bari, Bari, Italy

[70a]INFN Sezione di Bologna, Bologna, Italy

[70b]Università di Bologna, Bologna, Italy

[71a]INFN Sezione di Catania, Catania, Italy

[71b]Università di Catania, Catania, Italy

[72a]INFN Sezione di Firenze, Firenze, Italy

[72b]Università di Firenze, Firenze, Italy

[73]INFN Laboratori Nazionali di Frascati, Frascati, Italy

[74a]INFN Sezione di Genova, Genova, Italy

[74b]Università di Genova, Genova, Italy

[75a]INFN Sezione di Milano-Bicocca, Milano, Italy

[75b]Università di Milano-Bicocca, Milano, Italy

[76a]INFN Sezione di Napoli, Napoli, Italy

[76b]Università di Napoli 'Federico II', Napoli, Italy

[76c]Università della Basilicata, Potenza, Italy

[76d]*Università G. Marconi, Roma, Italy*

[77a]*INFN Sezione di Padova, Padova, Italy*

[77b]*Università di Padova, Padova, Italy*

[77c]*Università di Trento, Trento, Italy*

[78a]*INFN Sezione di Pavia, Pavia, Italy*

[78b]*Università di Pavia, Pavia, Italy*

[79a]*INFN Sezione di Perugia, Perugia, Italy*

[79b]*Università di Perugia, Perugia, Italy*

[80a]*INFN Sezione di Pisa, Pisa, Italy*

[80b]*Università di Pisa, Pisa, Italy*

[80c]*Scuola Normale Superiore di Pisa, Pisa, Italy*

[81a]*INFN Sezione di Roma, Rome, Italy*

[81b]*Sapienza Università di Roma, Rome, Italy*

[82a]*INFN Sezione di Torino, Torino, Italy*

[82b]*Università di Torino, Torino, Italy*

[82c]*Università del Piemonte Orientale, Novara, Italy*

[83a]*INFN Sezione di Trieste, Trieste, Italy*

[83b]*Università di Trieste, Trieste, Italy*

[84]*Kyungpook National University, Daegu, Korea*

[85]*Chonnam National University, Institute for Universe and Elementary Particles, Kwangju, Korea*

[86]*Hanyang University, Seoul, Korea*

[87]*Korea University, Seoul, Korea*

[88]*Kyung Hee University, Department of Physics, Seoul, Republic of Korea*

[89]*Sejong University, Seoul, Korea*

[90]*Seoul National University, Seoul, Korea*

[91]*University of Seoul, Seoul, Korea*

[92]*Yonsei University, Department of Physics, Seoul, Korea*

[93]*Sungkyunkwan University, Suwon, Korea*

[94]*College of Engineering and Technology, American University of the Middle East (AUM)*

[95]*Riga Technical University, Riga, Latvia*

[96]*Vilnius University, Vilnius, Lithuania*

[97]*National Centre for Particle Physics, Universiti Malaya, Kuala Lumpur, Malaysia*

[98]*Universidad de Sonora (UNISON), Hermosillo, Mexico*

[99]*Centro de Investigacion y de Estudios Avanzados del IPN, Mexico City, Mexico*

[100]*Universidad Iberoamericana, Mexico City, Mexico*

[101]*Benemerita Universidad Autonoma de Puebla, Puebla, Mexico*

[102]*Universidad Autónoma de San Luis Potosí, San Luis Potosí, Mexico*

[103]*University of Montenegro, Podgorica, Montenegro*

[104]*University of Auckland, Auckland, New Zealand*

[105]*University of Canterbury, Christchurch, New Zealand*

[106]*National Centre for Physics, Quaid-I-Azam University, Islamabad, Pakistan*

[107]*AGH University of Science and Technology Faculty of Computer Science,*
Electronics and Telecommunications, Krakow, Poland

[108]*National Centre for Nuclear Research, Swierk, Poland*

[109]*Institute of Experimental Physics, Faculty of Physics, University of Warsaw, Warsaw, Poland*

[110]*Laboratório de Instrumentação e Física Experimental de Partículas, Lisboa, Portugal*

[111]*Joint Institute for Nuclear Research, Dubna, Russia*

[112]*Petersburg Nuclear Physics Institute, Gatchina (St. Petersburg), Russia*

[113]*Institute for Nuclear Research, Moscow, Russia*

[114]*Institute for Theoretical and Experimental Physics named by A.I. Alikhanov of NRC*
'Kurchatov Institute', Moscow, Russia

[115]*Moscow Institute of Physics and Technology, Moscow, Russia*

[116]*National Research Nuclear University 'Moscow Engineering Physics Institute' (MEPhI),*
Moscow, Russia

[117]*P.N. Lebedev Physical Institute, Moscow, Russia*

[118]*Skobeltsyn Institute of Nuclear Physics, Lomonosov Moscow State University, Moscow, Russia*

[119]*Novosibirsk State University (NSU), Novosibirsk, Russia*

[120]*Institute for High Energy Physics of National Research Centre 'Kurchatov Institute', Protvino, Russia*

[121]*National Research Tomsk Polytechnic University, Tomsk, Russia*

[122]*Tomsk State University, Tomsk, Russia*

[123]*University of Belgrade: Faculty of Physics and VINCA Institute of Nuclear Sciences, Belgrade, Serbia*
[124]*Centro de Investigaciones Energéticas Medioambientales y Tecnológicas (CIEMAT), Madrid, Spain*
[125]*Universidad Autónoma de Madrid, Madrid, Spain*
[126]*Universidad de Oviedo, Instituto Universitario de Ciencias y Tecnologías Espaciales de Asturias (ICTEA), Oviedo, Spain*
[127]*Instituto de Física de Cantabria (IFCA), CSIC-Universidad de Cantabria, Santander, Spain*
[128]*University of Colombo, Colombo, Sri Lanka*
[129]*University of Ruhuna, Department of Physics, Matara, Sri Lanka*
[130]*CERN, European Organization for Nuclear Research, Geneva, Switzerland*
[131]*Paul Scherrer Institut, Villigen, Switzerland*
[132]*ETH Zurich—Institute for Particle Physics and Astrophysics (IPA), Zurich, Switzerland*
[133]*Universität Zürich, Zurich, Switzerland*
[134]*National Central University, Chung-Li, Taiwan*
[135]*National Taiwan University (NTU), Taipei, Taiwan*
[136]*Chulalongkorn University, Faculty of Science, Department of Physics, Bangkok, Thailand*
[137]*Cukurova University, Physics Department, Science and Art Faculty, Adana, Turkey*
[138]*Middle East Technical University, Physics Department, Ankara, Turkey*
[139]*Bogazici University, Istanbul, Turkey*
[140]*Istanbul Technical University, Istanbul, Turkey*
[141]*Istanbul University, Istanbul, Turkey*
[142]*Institute for Scintillation Materials of National Academy of Science of Ukraine, Kharkov, Ukraine*
[143]*National Scientific Center, Kharkov Institute of Physics and Technology, Kharkov, Ukraine*
[144]*University of Bristol, Bristol, United Kingdom*
[145]*Rutherford Appleton Laboratory, Didcot, United Kingdom*
[146]*Imperial College, London, United Kingdom*
[147]*Brunel University, Uxbridge, United Kingdom*
[148]*Baylor University, Waco, Texas, USA*
[149]*Catholic University of America, Washington, DC, USA*
[150]*The University of Alabama, Tuscaloosa, Alabama, USA*
[151]*Boston University, Boston, Massachusetts, USA*
[152]*Brown University, Providence, Rhode Island, USA*
[153]*University of California, Davis, Davis, California, USA*
[154]*University of California, Los Angeles, California, USA*
[155]*University of California, Riverside, Riverside, California, USA*
[156]*University of California, San Diego, La Jolla, California, USA*
[157]*University of California, Santa Barbara—Department of Physics, Santa Barbara, California, USA*
[158]*California Institute of Technology, Pasadena, California, USA*
[159]*Carnegie Mellon University, Pittsburgh, Pennsylvania, USA*
[160]*University of Colorado Boulder, Boulder, Colorado, USA*
[161]*Cornell University, Ithaca, New York, USA*
[162]*Fermi National Accelerator Laboratory, Batavia, Illinois, USA*
[163]*University of Florida, Gainesville, Florida, USA*
[164]*Florida International University, Miami, Florida, USA*
[165]*Florida State University, Tallahassee, Florida, USA*
[166]*Florida Institute of Technology, Melbourne, Florida, USA*
[167]*University of Illinois at Chicago (UIC), Chicago, Illinois, USA*
[168]*The University of Iowa, Iowa City, Iowa, USA*
[169]*Johns Hopkins University, Baltimore, Maryland, USA*
[170]*The University of Kansas, Lawrence, Kansas, USA*
[171]*Kansas State University, Manhattan, Kansas, USA*
[172]*Lawrence Livermore National Laboratory, Livermore, California, USA*
[173]*University of Maryland, College Park, Maryland, USA*
[174]*Massachusetts Institute of Technology, Cambridge, Massachusetts, USA*
[175]*University of Minnesota, Minneapolis, Minnesota, USA*
[176]*University of Mississippi, Oxford, Mississippi, USA*
[177]*University of Nebraska-Lincoln, Lincoln, Nebraska, USA*
[178]*State University of New York at Buffalo, Buffalo, New York, USA*
[179]*Northeastern University, Boston, Massachusetts, USA*
[180]*Northwestern University, Evanston, Illinois, USA*
[181]*University of Notre Dame, Notre Dame, Indiana, USA*

[182]The Ohio State University, Columbus, Ohio, USA

[183]Princeton University, Princeton, New Jersey, USA

[184]University of Puerto Rico, Mayaguez, Puerto Rico, USA

[185]Purdue University, West Lafayette, Indiana, USA

[186]Purdue University Northwest, Hammond, Indiana, USA

[187]Rice University, Houston, Texas, USA

[188]University of Rochester, Rochester, New York, USA

[189]Rutgers, The State University of New Jersey, Piscataway, New Jersey, USA

[190]University of Tennessee, Knoxville, Tennessee, USA

[191]Texas A&M University, College Station, Texas, USA

[192]Texas Tech University, Lubbock, Texas, USA

[193]Vanderbilt University, Nashville, Tennessee, USA

[194]University of Virginia, Charlottesville, Virginia, USA

[195]Wayne State University, Detroit, Michigan, USA

[196]University of Wisconsin—Madison, Madison, WI, Wisconsin, USA

[a]Deceased.

[b]Also at Vienna University of Technology, Vienna, Austria.

[c]Also at Institute of Basic and Applied Sciences, Faculty of Engineering, Arab Academy for Science, Technology and Maritime Transport.

[d]Also at Université Libre de Bruxelles, Bruxelles, Belgium.

[e]Also at IRFU, CEA, Université Paris-Saclay, Gif-sur-Yvette, France.

[f]Also at Universidade Estadual de Campinas, Campinas, Brazil.

[g]Also at Federal University of Rio Grande do Sul, Porto Alegre, Brazil.

[h]Also at Federal University of Mato Grosso do Sul (UFMS) Campo Grande, Mato Grosso do Sul, Brazil.

[i]Also at Universidade Federal de Pelotas, Pelotas, Brazil.

[j]Also at University of Chinese Academy of Sciences, Beijing, China.

[k]Also at Institute for Theoretical and Experimental Physics named by A.I. Alikhanov of NRC 'Kurchatov Institute', Moscow, Russia.

[l]Also at Joint Institute for Nuclear Research, Dubna, Russia.

[m]Also at Zewail City of Science and Technology, Zewail, Egypt.

[n]Also at Helwan University, Cairo, Egypt.

[o]Also at Ain Shams University, Cairo, Egypt.

[p]Also at Purdue University, West Lafayette, Indiana, USA.

[q]Also at Université de Haute Alsace, Mulhouse, France.

[r]Also at Tbilisi State University, Tbilisi, Georgia.

[s]Also at Erzincan Binali Yildirim University, Erzincan, Turkey.

[t]Also at CERN, European Organization for Nuclear Research, Geneva, Switzerland.

[u]Also at RWTH Aachen University, III. Physikalisches Institut A, Aachen, Germany.

[v]Also at University of Hamburg, Hamburg, Germany.

[w]Also at Department of Physics, Isfahan University of Technology, Isfahan, Iran.

[x]Also at Brandenburg University of Technology, Cottbus, Germany.

[y]Also at Skobeltsyn Institute of Nuclear Physics, Lomonosov Moscow State University, Moscow, Russia.

[z]Also at Institute of Physics, University of Debrecen, Debrecen, Hungary.

[aa]Also at Physics Department, Faculty of Science, Assiut University, Assiut, Egypt.

[bb]Also at MTA-ELTE Lendület CMS Particle and Nuclear Physics Group, Eötvös Loránd University, Budapest, Hungary.

[cc]Also at Institute of Nuclear Research ATOMKI, Debrecen, Hungary.

[dd]Also at IIT Bhubaneswar, Bhubaneswar, India.

[ee]Also at Institute of Physics, Bhubaneswar, India.

[ff]Also at G.H.G. Khalsa College, Punjab, India.

[gg]Also at Shoolini University, Solan, India.

[hh]Also at University of Hyderabad, Hyderabad, India.

[ii]Also at University of Visva-Bharati, Santiniketan, India.

[jj]Also at Indian Institute of Technology (IIT), Mumbai, India.

[kk]Also at Deutsches Elektronen-Synchrotron, Hamburg, Germany.

[ll]Also at Department of Physics, University of Science and Technology of Mazandaran, Behshahr, Iran.

[mm]Also at INFN Sezione di Bari, Università di Bari, Politecnico di Bari, Bari, Italy.

[nn]Also at Italian National Agency for New Technologies, Energy and Sustainable Economic Development, Rome, Italy.

[oo]Also at Centro Siciliano di Fisica Nucleare e di Struttura Della Materia, Catania, Italy.

[pp]Also at Riga Technical University, Riga, Latvia.

[qq]Also at Consejo Nacional de Ciencia y Tecnología, Mexico City, Mexico.

[rr]Also at Warsaw University of Technology, Institute of Electronic Systems, Warsaw, Poland.

[ss]Also at Institute for Nuclear Research, Moscow, Russia.

[tt]Also at National Research Nuclear University 'Moscow Engineering Physics Institute' (MEPhI), Moscow, Russia.

[uu]Also at St. Petersburg State Polytechnical University, St. Petersburg, Russia.

[vv]Also at University of Florida, Gainesville, Florida, USA.

[ww]Also at Imperial College, London, United Kingdom.

[xx]Also at P.N. Lebedev Physical Institute, Moscow, Russia.

[yy]Also at California Institute of Technology, Pasadena, California, USA.

[zz]Also at Budker Institute of Nuclear Physics, Novosibirsk, Russia.

[aaa]Also at Faculty of Physics, University of Belgrade, Belgrade, Serbia.

[bbb]Also at Università degli Studi di Siena, Siena, Italy.

[ccc]Also at Trincomalee Campus, Eastern University, Sri Lanka.

[ddd]Also at INFN Sezione di Pavia, Università di Pavia, Pavia, Italy.

[eee]Also at National and Kapodistrian University of Athens, Athens, Greece.

[fff]Also at Universität Zürich, Zurich, Switzerland.

[ggg]Also at Stefan Meyer Institute for Subatomic Physics, Vienna, Austria.

[hhh]Also at Laboratoire d'Annecy-le-Vieux de Physique des Particules, IN2P3-CNRS, Annecy-le-Vieux, France.

[iii]Also at Şırnak University, Şırnak, Turkey.

[jjj]Also at Department of Physics, Tsinghua University, Beijing, China.

[kkk]Also at Near East University, Research Center of Experimental Health Science, Nicosia, Turkey.

[lll]Also at Beykent University, Istanbul, Turkey.

[mmm]Also at Istanbul Aydin University, Application and Research Center for Advanced Studies (App. & Res. Cent. for Advanced Studies), Istanbul, Turkey.

[nnn]Also at Mersin University, Mersin, Turkey.

[ooo]Also at Piri Reis University, Istanbul, Turkey

[ppp]Also at Adiyaman University, Adiyaman, Turkey.

[qqq]Also at Ozyegin University, Istanbul, Turkey.

[rrr]Also at Izmir Institute of Technology, Izmir, Turkey.

[sss]Also at Necmettin Erbakan University, Konya, Turkey.

[ttt]Also at Bozok Universitetesi Rektörlügü.

[uuu]Also at Marmara University, Istanbul, Turkey.

[vvv]Also at Milli Savunma University, Istanbul, Turkey.

[www]Also at Kafkas University, Kars, Turkey.

[xxx]Also at Istanbul Bilgi University, Istanbul, Turkey.

[yyy]Also at Hacettepe University, Ankara, Turkey.

[zzz]Also at Vrije Universiteit Brussel, Brussel, Belgium.

[aaaa]Also at School of Physics and Astronomy, University of Southampton, Southampton, United Kingdom.

[bbbb]Also at IPPP Durham University, Durham, United Kingdom.

[cccc]Also at Monash University, Faculty of Science, Clayton, Australia.

[dddd]Also at Bethel University, St. Paul, Minneapolis, USA.

[eeee]Also at Karamanoğlu Mehmetbey University, Karaman, Turkey.

[ffff]Also at Bingol University, Bingol, Turkey.

[gggg]Also at Georgian Technical University, Tbilisi, Georgia.

[hhhh]Also at Sinop University, Sinop, Turkey.

[iiii]Also at Mimar Sinan University, Istanbul, Istanbul, Turkey.

[jjjj]Also at Nanjing Normal University Department of Physics, Nanjing, China.

[kkkk]Also at Texas A&M University at Qatar, Doha, Qatar.

[llll]Also at Kyungpook National University, Daegu, Korea.